IMPROVED PERFORMANCE OF A RADIO FREQUENCY IDENTIFICATION TAG ANTENNA ON A METAL GROUND PLANE

A Thesis
Presented to
The Academic Faculty

by

Joel Thomas Prothro

In Partial Fulfillment
of the Requirements for the Degree
Master of Science in the
School of Electrical and Computer Engineering

Georgia Institute of Technology
August 2007

IMPROVED PERFORMANCE OF A RADIO FREQUENCY IDENTIFICATION TAG ANTENNA ON A METAL GROUND PLANE

Approved by:

Professor Gregory D. Durgin, Adviser
School of Electrical and Computer Engineering
Georgia Institute of Technology

Professor Bernard Kippelen
School of Electrical and Computer Engineering
Georgia Institute of Technology

Professor Andrew Peterson
School of Electrical and Computer Engineering
Georgia Institute of Technology

Date Approved: 15 May, 2007

To my parents, Sam and Nancy Prothro, for their love and support throughout my continued education.

ACKNOWLEDGEMENTS

Special thanks to my advisor, Gregory Durgin for his inspiration and continued support throughout this project. Thanks for challenging me to go further than I thought I could. Also thanks to Joshua Griffin, whose work inspired this research. And thanks to the Sampei Laboratory in Osaka, Japan, for allowing me to learn in such a special environment.

TABLE OF CONTENTS

LIST OF TABLES

LIST OF FIGURES

SUMMARY

Although RFID is quickly gaining popularity in consumer and engineering circles, its current state severely limits its usage to specifically designed, highly controlled environments. This work explores a large barrier to widespread RFID implementation: antenna performance degradation due to a metal ground plane, and suggests ways to improve the performance. The theoretical physics of the performance degradation is explored. Simulations and measurements were taken to explore actual performance degradations. Experimental antennas were designed and fabricated, and a carefully calibrated experimental system was used to measure the antenna properties at many different antenna–ground plane separation distances between 0.6cm and 2.9cm.

Based on the previous experiments, another set of experiments was taken in an effort to explore ways of electromagnetically moving the antenna away from the ground plane. A dielectric spacer was used to decrease the wavelength of the incoming signal so the antenna would appear electromagnetically far from the ground plane. Although these measurements showed a decrease in radiation efficiency, they also showed an increase in impedance. Based on these measurements a high permittivity and high permeability spacer is suggested and explored. This spacer would allow the impedance to be increased while not hindering the antenna radiation efficiency.

CHAPTER I

INTRODUCTION

Consumer interest in radio frequency identification (RFID) has sharply increased in the last several years; however, if existing problems remain unsolved, the endless possibilities for RFID will never be a reality, and the current, severely limited applications will be the unfortunate pinnacle of this promising technology. Engineers and scientists are researching RFID and other backscatter radio systems trying to create a cohesive technology deployable in a variety of enviroments. The "holy grail" of RFID technology is the replacement of item bar codes with RF tags. This research will address a core inhibitor to widespread implementation: antenna performance degradation when placed on a metalic surface when operating in the far field in the UHF band. Also offered in this research is a solution to the problem that will allow the RFID tag to operate reliably regardless of what is attached to the tag.

When an antenna comes close to a high-dielectric or a high-conductivity object, the antenna impedance and the ability to couple power onto the antenna are adversely affected. In a passive system, if power cannot be efficiently coupled onto the antenna, the read range will be very small and the tag will not be able to function as a part of a reliable link. Nikitin in [9] shows that if just 10dB is lost from the link due to material attachment, the read range will decrease by about 60 percent. Even when sufficient power arrives at the tag, if the impedance of the tag antenna drops too low, backscatter modulation cannot be received and decoded by the reader. Without a solution to these problems, RFID will never be a reliable alternative to the ubiquitous bar code, and RFID will be restricted for use in specific environments.

Consider the implications for radio communications if an antenna system could

be designed that functioned reliably without regard to antenna material attachment. Not only would RFID be revolutionized, but all small device wireless communication would take a giant leap forward.

Other work has been done testing read ranges of commercial RFID tags placed on typical objects [3]. Still others have simulated the effects the ground plane has on the tag [14], but this work will address the electromagnetic problem from three different areas: theory, simulation, and experimentation. Finally this work will demonstrate through experiment solutions to the antenna performance problems.

1.1 Common RFID Implementations

All RFID systems are implemented with two basic components, a reader and a tag. A schematic is shown in Figure 1 of a RFID system. In general, the reader sends a signal to the tag, and the tag responds to the reader by sending its identification code. The RFID reader also generally has two components, the transmitting hardware and the receiving hardware. Although these are separate components, the RFID reader can use a single antenna for transmitting and receiving the signal. The RFID reader can also be two separate entities with the transmitter hardware and receiver hardware in different locations. The RFID tag is composed of two basic components as well:

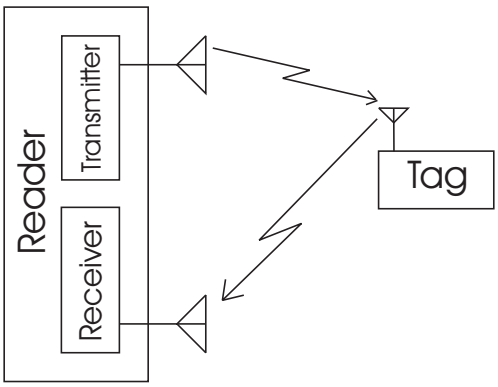

Figure 1: Typical RFID system schematic of a reader (left), consisting of a transmitter and receiver unit, and an RF tag (right) that backscatters information.

the antenna, which is used to receive and transmit, and the RF integrated circuit

(RFIC) chip, which encodes and modulates the identification information through the antenna. Within this basic structure, engineers have developed many ways to create an RFID link.

1.1.1 Near-Field RFID

Most commonly operating in the 13.56MHz band, near-field RFID has been in commercial use for many years and has served a variety of markets. Finding applications in markets from livestock inventory to vehicle security [10], near-field RFID has transformed communication applications that require physical proximity by creating a contact free communications scheme. For near-field tags to operate, they must be physically close to the reader, generally less than one meter. Near-field systems operate using magnetic coupling where the coil (antenna) of the tag is excited by the magnetic field of the coil (antenna) of the reader. Figure 2 shows a typical near-field tag design. After excitation, the tag sends the identification code to the reader. The long wavelength of near-field systems make them very efficient regardless of what is attached to them. The signal travels through many non-metallic substances without much loss, and, due to the relatively long wavelength, it travels around most non-penetrable substances such as water and metal. This makes near-field RFID a very

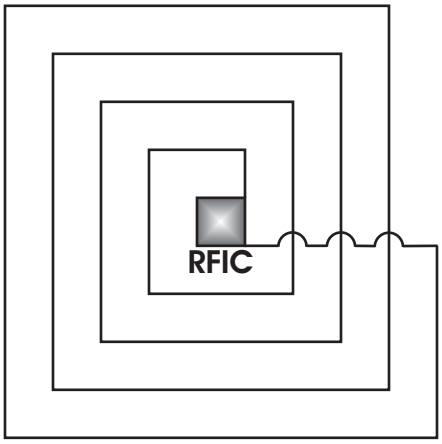

Figure 2: Typical near-field antennas consist of inductive loops.

attractive option if the application can survive with read distances under one meter.

1.1.2 Far-Field RFID

Although far- and near-field RFID use the same basic algorithm at the system level, their implementation is very different. Far-field RFID uses traveling waves to send and receive information. The far-field is generally defined as the area where incident waves can be accurately modeled as plane waves. For an antenna to be in the far field, it must be at distance which satisfies equation (1) where D is the largest dimension of the reader antenna.

$$d > \max\left(\lambda, \frac{D^2}{\lambda}\right) \tag{1}$$

Far-field RFID has currently found application is such things as highway toll collection, inventory management, and assembly line automation. The draw of the far-field RFID system is that a tag can be read without being in close physical proximity to the reader. Far-field RFID is usually implemented using higher frequency signals because the antenna size for a low frequency signal is too big to be feasible for many RFID applications (e.g. a half wave dipole for 13.56MHz signal is approximately 22 meters); therefore, far-field RFID research is concentrated in the UHF and microwave bands – most commonly in the unlicensed Industrial-Scientific-Medical (ISM) bands of 915MHz, 2.4GHz and 5.4GHz. Unfortunately, UHF and microwave frequency antennas are also very susceptible to material attachment degradations [6], making it very difficult to tag high-dielectric or high-conductivity objects.

1.1.3 Active versus Passive Tags

Both near- and far-field tags can either be active or passive–where an active tag denotes a tag that has an internal power source, and a passive tag denotes a tag that does not have an internal power source, but rather, receives its energy from the incoming wave. The basic active and passive classes have subclasses, such as

power scavenging tags and semi-active tags, but the focus in this research will be on battery powered active tags and purely passive tags. Factors that distinguish tags are summarized below:

- **Chip complexity:** An active tag can have much more complex computational ability. Active tags could even be complete DSP-enabled transceivers. The chip on a passive tag is limited because it receives very little power from the incoming wave.

- **Tag range:** Since the active tag has external power, it has the ability to transmit a signal much further than a purely passive tag.

- **Cost:** The battery of an active tag will make it more expensive than a passive tag. The battery could easily become the most expensive part of the tag.

- **Size:** A passive tag can be much smaller than an active tag using current battery technology. Without the antenna, a passive tag is micrometers thick and is only a few millimeters wide.

- **Shelf life:** Since battery life is limited, the shelf life of an active tag is also limited. The passive tag can theoretically have an unlimited shelf life.

CHAPTER II

PASSIVE FAR-FIELD RFID TAGS

This research will focus on passive, far-field RFID tags, although the results are equally valid for active tags. Passive, far-field RFID tags operate in the far-field of the reader antennas and gather all of their energy from the incoming electromagnetic signal. They are chosen because, if a few engineering difficulties can be overcome, the long read range and unlimited shelf life make them the most versatile. This research will suggest a solution to one of the most common and basic problems with far-field tags: antenna performance degradations due to material attachment.

2.1 Passive RFID Operation

Passive RFID works by using backscatter modulation; originally proposed by Stockman [3], backscatter modulation transmits information by changing relative impedance of the chip to the impedance of the antenna. The general method is shown in Figure 3 and outlined below:

- The reader interrogates the tag with a continuous wave (CW) signal.
- The tag uses the incoming electromagnetic energy to power up and operate.
- The tag modulates its pre-programmed code by changing its relative impedance value causing a modulated reflection of the CW signal.

To modulate the information, the passive tag switches between a very high impedance and a relatively matched load. In the matched case, most of the power from the incoming CW signal is absorbed by the chip and very little power is reflected back to the reader. Ideally in the high impedance case, the mismatch between the chip and

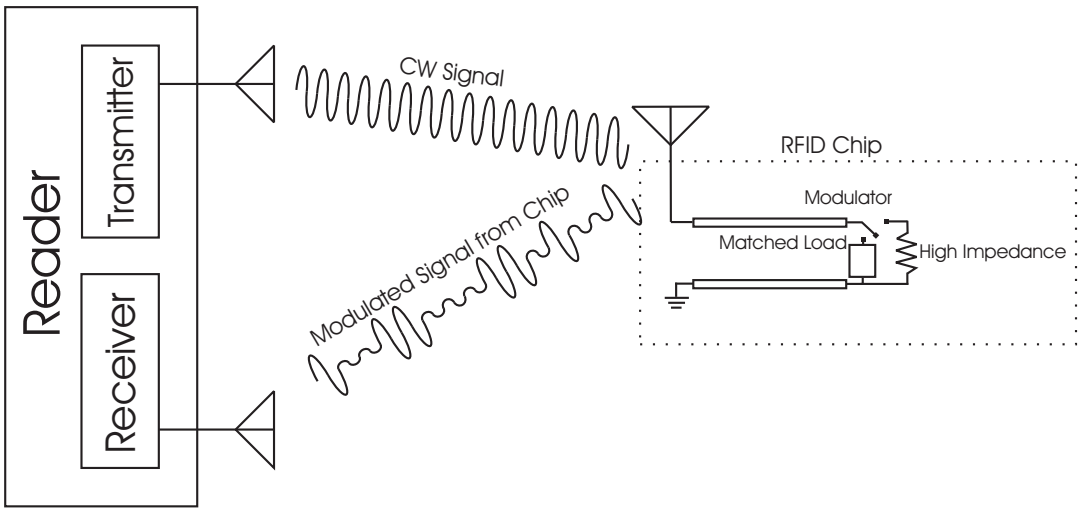

Figure 3: RFID using backscatter modulation consists of a reader and a tag. The reader sends on a CW signal and the modulates that signal with the information and reflects it back.

the antenna would reflect all of the power back to the reader; however, the chip needs to continuously absorb energy from the reader in order to stay powered, so according to EPC Global standards, the "antenna modulation shall maximally be 30% drop in RF port voltage over full input power range to allow the chip to maintain power for operation" [4]; therefore, passive RFID uses amplitude shift keying to transmit information. These design specifications impose two very important design criteria on the engineer.

1. The incoming signal must be efficiently coupled onto the antenna and then the chip because of the difficulty of powering the chip with the CW signal. Although the chip does not need much power to operate (Karthaus and Fischer designed an RFIC which required only 30μW [7]), the incoming power for the CW signal is very low, so all of the possible power must be harnessed for this passive device. Lack of available energy for power-up is often the limiting factor for the range of the RFID tag.

2. The antenna impedance needs to be high enough to allow the chip to reliably modulate information onto the antenna. Many chip designers use either

a transistor or a PIN diode to create the matched and high impedance circuits; however, neither pin diode nor a transistor can create an impedance perfectly matched to the antenna. It is necessary that the antenna impedance, Z_a, be as high as the modulation circuitry's lowest possible impedance. The antenna impedance must also be high enough that a slight error in matching the impedance does not cause the system to fail. For example, consider the case when the matching circuitry impedance, Z_t, misses the match by 2Ω. According to equation (2), if the antenna's impedance is 50Ω, there is an almost perfect match (only a 2% mismatch).

$$\Gamma = \frac{Z_{\mathrm{t}} - Z_{\mathrm{a}}}{Z_{\mathrm{t}} + Z_{\mathrm{a}}} \tag{2}$$

Now assume the antenna's impedance is 3Ω; if the PIN diode again missed matching the antenna by 2Ω, the mismatch would be 20% instead of 2%, making the link highly inefficient.

2.1.1 Modulation Using PIN Diode

A PIN diode is often used to modulate the impedance with the encoded information. PIN diodes are similar to PN diodes except there is a small intrinsic region between the P and the N regions. This allows for high frequency operation and more precise impedance control. Figure 4 shows the IV curve for a PIN diode. When a PIN diode has a reverse DC bias, it has a very high impedance, but when the PIN diode is forward DC biased, it behaves as a short circuit that can be connected to a matched load; therefore, to modulate the impedance, all the chip needs to do is modulate the DC bias of the PIN diode.

2.1.2 Power Harvesting

The RF signal received at the tag has very little power, not nearly enough power to run the tag if only a single rectifier circuit is used. To harvest enough power from

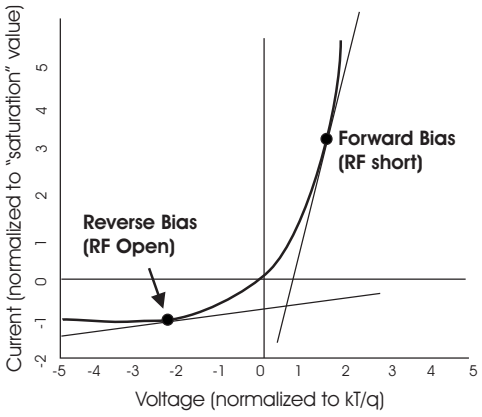

Figure 4: The IV curve of a PIN diode showing how the output of the diode varies according to bias.

the incoming signal, a voltage multiplier is often used. Figure 5 shows a schematic for an RF voltage doubler circuit. When the sinusoidal RF signal is positive, the voltage of the RF signal charges the capacitor to the right. When the sinusoidal voltage is negative, charge is stored on the capacitor to the left; therefore, when the circuit reaches steady state, there is a DC voltage drop across each diode, resulting in an amplitude that is twice that of the sinusoidal signal (minus the turn on voltage for the diodes). In the case of passive RFID, the chip needs even more power than double the incoming signal, but the voltage doublers can be concatenated to create a multi-stage voltage multiplier.

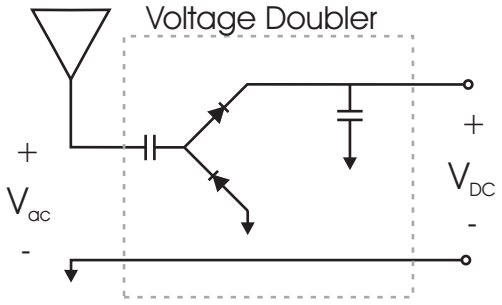

Figure 5: Schematic of a voltage doubler. A concatenation of voltage doublers is used to to power passive RFID tags.

2.2 Material Attachment

Antennas do not operate independently of the objects near them; rather, neighboring objects to varying degrees affect the radiation properties of the antenna. Engineers have used this fact to improve the performance of many different antennas. For example, reflectors are often strategically placed to increase the directivity of an antenna; however, when many substances, especially metal, come very close to an antenna, the antenna becomes inoperable. For "peel and stick" RFID systems to have maximum usefulness, the material the tag is attached to should have minimal effect on the performance of the tag.

2.3 Metal Attachment

For any perfect electric conducting plane, the tangential component of electric field, $\vec{E}$ is zero at any point on the surface of the conductor.

$$\hat{n} \times \vec{E} = \vec{0} \tag{3}$$

Where $\hat{n}$ is a unit vector normal to the metallic surface. Therefore, when the electric field caused by a nearby antenna contacts the PEC, reverse currents are excited on the surface plane that cancel out the tangential component of electric field at the surface of the plane. The effect of the ground plane only cancels the electric field on the surface of the ground plane, not elsewhere in space; therefore, a ground plane placed a quarter wavelength away from the antenna will cause the transmitted wave to have a 360 degree phase shift when it returns to the antenna. This will cause constructive interference and give the antenna more directivity. However, when the metal-antenna separation distance is much less than a quarter of a wavelength, the antenna properties begin to suffer because the reflected wave has a phase shift approaching 180 degrees, and a phase shift of 180 degrees causes total destructive interference with the signal coming directly from the antenna.

The interference of the ground plane can also be described using the method of images [17]. In this context, the method of images states that the ground plane can be replaced with an antenna with currents exactly opposite the currents of the original antenna, as shown in Figure 6.

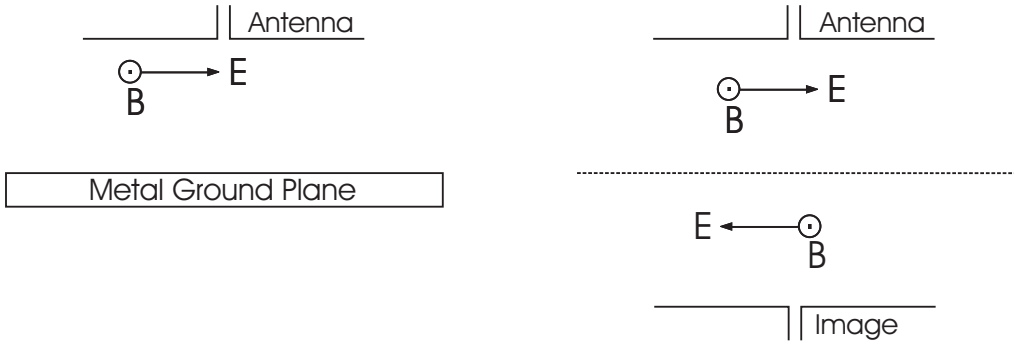

Figure 6: An illustrative example of the method of images. An antenna approaching a metallic surface (left) is equivalent to two antennas – primary and image – in free space (right).

The method of images requires that the ground plane be of infinite dimension and a perfect electric conductor. Although an RFID tag will never be placed on an infinite PEC, this is a good approximation for two reasons. First, most metals are accurately approximated as perfect electric conductors at RF, and second, as the distance between the antenna and the ground plane becomes very small, the ground plane dimensions begin to look infinite if the ground plane is larger than the antenna. The larger the ground plane, the sooner it begins to look infinite with reference to the separation distance of the antenna.

Recall for a passive RFID system to work, it needs to get as much power as possible from the incoming wave. Since these reflections are taking place, very little power from the incoming signal is being coupled into the chip, and very little of the modulated signal can be reflected from the chip antenna.

2.3.1 Link Budget

The power received by the tag antenna from the transmitter antenna can be described by the Friis link budget, equation (4), which is given in the logarithmic form.

$$P_{\text{tag}} = P_{\text{reader-tx}} - L_{\text{sys}} + G_{\text{reader-tx}} + G_{\text{tag}} - 20\log_{10}\left(\frac{4\pi}{\lambda}\right) - 20\log_{10}(d) \quad (4)$$

where

P_{tag} (dB)	–	power at the RF tag antenna terminals
$P_{\text{reader-tx}}$ (dB)	–	power input to the reader transmit antenna
L_{sys} (dB)	–	polarization and system losses in the receiver and tag
$G_{\text{reader-tx}}$ (dB)	–	gain of the reader transmit antenna
G_{tag} (dB)	–	RF tag antenna gain in free space
$20\log_{10}\left(\frac{4\pi}{\lambda}\right)$	–	a loss dependent upon the freespace wavelength, λ
$20\log_{10}(d)$	–	free space path loss referenced to 1 m

Griffin et al. in [6] extended the Friis transmission equation to include the gain penalty (GP) for placing an antenna on an object. For the forward link required to power the tag the Friis equation becomes equation (5).

$$P_{\text{tag}} = P_{\text{reader-tx}} - L_{\text{sys}} + G_{\text{reader-tx}} + G_{\text{tag}} - GP - 20\log_{10}\left(\frac{4\pi}{\lambda}\right) - 20\log_{10}(d) \quad (5)$$

For the backscatter link, Griffin adds the mismatch due to the modulation circuitry, Γ. Therefore, the linear link budget becomes equation (6).

$$P_{\text{reader-rx}} = \frac{P_{\text{reader-tx}}\, G_{\text{reader-tx}}\, G_{\text{reader-rx}}\, G_{\text{tag}}^2\, |\Gamma|^2\, \lambda^4}{L_{\text{sys}}\, d^4\, (4\pi)^2\, GP^2} = \xi_{\text{link}}\, |\Gamma|^2 \quad (6)$$

For data, the link budget is dependent on both states. Consider the case where Γ_A is the reflection coefficient for symbol A and Γ_B is the reflection coefficient for symbol B. $\Gamma_{A,B}$ is defined in (7).

$$\Gamma_{A,B} = \frac{Z_{A,B} - Z_o^*}{Z_{A,B} + Z_o} \tag{7}$$

So the voltages at the reader are dependent on Γ_A and Γ_B, as given in (8) and (9).

$$V_{\text{rx,A}} = \sqrt{\xi_{\text{link}}}\, \Gamma_A \ \exp(j\ \Phi_{\text{channel}}) \tag{8}$$

$$V_{\text{rx,B}} = \sqrt{\xi_{\text{link}}}\, \Gamma_B \ \exp(j\ \Phi_{\text{channel}}) \tag{9}$$

The data switches between loads A and B depending on the transmitted binary sequence. In a standard RFID reader, the signal passes through a DC block, removing the DC component, so assuming an equal number of ones and zeros the voltage can be described by equations (10) and (11).

$$V_{\text{rx(DC)}} = \frac{\sqrt{\xi_{\text{link}}}}{2}\ (\Gamma_A + \Gamma_B)\ \exp\left(j\ \Phi_{\text{channel}}\right) \tag{10}$$

$$V_{\text{rx(DATA)}} = \frac{\sqrt{\xi_{\text{link}}}}{2}\ (\Gamma_A - \Gamma_B)\ \exp\left(j\ \Phi_{\text{channel}}\right) \tag{11}$$

Writing A and B in terms of the DC value produces

Symbol A: $V_{\text{rx(DC)}} + V_{\text{rx(DATA)}}$ and

Symbol B: $V_{\text{rx(DC)}} - V_{\text{rx(DATA)}}$.

Therefore, the link budget for data becomes equation (12).

$$P_{\text{reader-rx}} = \frac{\xi_{\text{link}}}{4}|\Gamma_A - \Gamma_B|^2 = \frac{P_{\text{reader-tx}}\ G_{\text{reader-tx}}\ G_{\text{reader-rx}}\ G_{\text{tag}}^2\ |\Gamma_A - \Gamma_B|^2\ \lambda^4}{4\ L_{\text{sys}}\ d^4\ (4\pi)^2\ GP^2} \tag{12}$$

Note in equation (12) that the gain penalty GP for the data link budget becomes very important as the term is counted twice on the dB scale.

2.3.2 Impedance

Another problem caused by moving the antenna close to a metal plate is the decrease of impedance. As the antenna moves very close, the impedance can drop too low to effectively modulate the signal. The impedance of the antenna is proportional to the

electric field divided by the magnetic field. As the antenna is moved close to the PEC, the electric field goes to zero. Not mentioned to this point is the fact that although the electric field cancels out because of a 180 degree phase shift, the magnetic field reflects with no phase shift, so it is constructively interfering; therefore, the effective impedance defined in equation (13) quickly goes to zero as the antenna is moved towards the ground plane.

$$Z \propto \frac{|\vec{E}|}{|\vec{H}|} \tag{13}$$

As an example, consider a wave propagating in the $\hat{z}$ direction normally incident on a perfectly conducting xy plane. The incident electric field, $\vec{E}$, only has components in the $\hat{x}$ directions, and the magnetic field, $\vec{H}$ only has components in the $\hat{y}$ direction; therefore, the wave is propagating in the $\hat{z}$ direction.

$$\hat{x} \times \hat{y} = \hat{z} \tag{14}$$

Since the electric field on the surface of a PEC must be zero, the reflected electric field is the negative of the incident field, and the wave begins to travel in the $-\hat{z}$ direction. This leads to a reflected wave equation in the form of (15).

$$-\hat{x} \times \hat{y} = -\hat{z} \tag{15}$$

When the incident and reflected waves are added together, the electric field goes to zero and the magnetic field doubles.

$$E_i + E_r = E_i + (-E_i) = 0 \tag{16}$$

$$H_i + H_r = H_i + H_i = 2H_i \tag{17}$$

Therefore, the impedance of equation (13) quickly goes to zero.

2.4 Antenna Design

The design of the antenna is a very important part of the RFID tag design. Many design constraints are placed on the RF engineer for the RFID tag antenna.

- **Performance:** The antenna must be able to perform reliably not only in free space, but also when attached to a variety of different materials.
- **Cost:** The RFID antenna must be very cheap if RFID tags are to replace bar codes on the item level.
- **Size:** The antenna's footprint must be small. It is also desirable for the tag to have a very low profile. [13]

RFID antennas are measured based on the above factors, and many designs have been developed in an effort to meet these constraints.

2.4.1 Patch Antennas

Although not originally designed for RFID, patch antennas have become a popular option in the literature for the RFID tag. Shown in Figure 7, their common use in other small electronic devices make them a viable candidate for RFID antennas. Patch antennas are generally designed on a microchip by placing a small metal plate on a dielectric substrate. The plate is excited with an RF signal fed from a microstrip line. The patch radiates the signal into space. When placed very close to a ground plane, the patch antenna generally performs better than a dipole design because the patch can be designed so the ground plane improves the radiation performance; however, the patch antenna has several disadvantages. Patch antennas generally have a very narrow bandwidth and require precise fabrication in order to function at the desired frequency. Also, both sides of the dielectric must have metal on them, causing difficulty in fabrication and added expense. They are also require a non-trivial thickness and most are brittle – eliminating the possibility of "peel-and-stick."

2.4.2 Perfect Magnetic Conductors

The idea of a perfect magnetic conductor (PMC) has existed in theory and has long been used in the study of electromagnetics. The PMC is the dual of the PEC where the boundary condition is $\hat{n} \times \vec{H} = \vec{0}$ instead of $\hat{n} \times \vec{E} = \vec{0}$. Although a true PMC does not exist in nature, engineers have developed ways to create surfaces that behave similar to a PMC over a specified bandwidth. Since the PMC reflects incoming electric waves without a phase

change, the PMC would be a good solution to the problem of destructive interference as the antenna moves very close to the ground plane; therefore, the PMC could be used as barrier between the antenna and the PEC ground plane.

In practice, electromagnetic band-gap (EBG) structures are used to mimic PMC planes. Many EBG structures are three dimensional consisting of a ground plane, a dielectric substrate and a periodic lattice [12]; however, Ma et al. showed that a two dimensional structure could be built that resembled a PMC ground plane [8].

Much work has been done with the hope of creating an antenna system that used the properties of an EBG to improve antenna performance. Orton and Seddon in [11] measured the effect of placing an EBG structure between an dipole antenna and a metal ground plane, and they found the impedance was higher than if the EBG structure had not been used. Best and Hanna in [1] developed a broadband radiator with an EBG substrate that could operate very close to a metal ground plane.

The main problem with using EBG structures in RFID application is their narrow bandwidth [12] and the difficulty of their design and manufacture. For example, Best in [1] created a broad band antenna using an EBG, but his structure requires metal vias drilled into a dielectric with a non-trivial thinkness. The bandwidth of EBG structures is often so small that a slight error in fabrication can cause the system to resonate outside of the desired frequency.

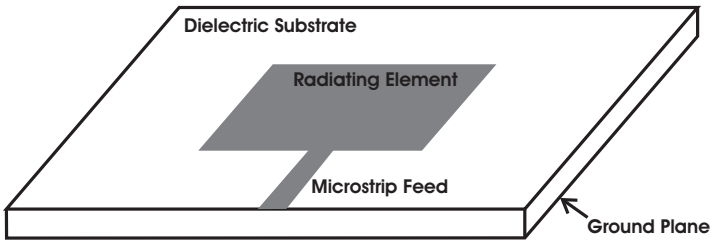

Figure 7: A typical patch antenna consists of a metal patch on a dielectric substrate fed with a microstrip line. The bottom of the dielectric is metallic and acts as a ground plane.

2.4.3 Planar Inverted-F Antennas

A planar inverted-f antenna (PIFA), Figure 8, is basically a patch antenna with a shorting plane connecting the patch to the ground plane. The advantage of a PIFA over a traditional patch antenna is a smaller size and greater VSWR bandwidth. Although the PIFA antenna

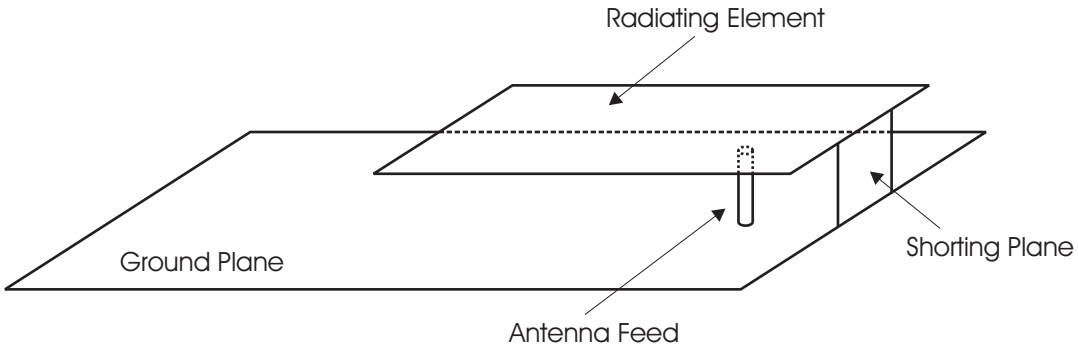

Figure 8: A basic PIFA antenna is similar to the patch antenna except it is commonly fed by a feeding pin drilled through the dielectric. The plate is also shorted to the ground plane.

has some favorable characteristics it is limited by its narrow bandwidth and its difficulty in implementing in RFID systems. Many designs are being studied to increase the bandwidth of the PIFA, and as PIFA properties are improved, the design and structure of the antenna becomes very complex [2], and difficult and costly to fabricate. Regardless of how high researchers can extend the bandwidth, the shorting plate requires an electrical connection be made between the PIFA and the ground plane, so the PIFA must either have its own ground plane or be electrically attached to the object it is tagging. PFIAs at 915MHz also have a thickness of around 5mm, making these rigid designs suffer from many of the same drawbacks as the traditional patch.

2.4.4 Other Designs

Many other designs have been proposed in the literature, but most fall into one of the basic categories described above. Dipoles have been tuned to work at a specific height above the ground plane [16]. Addition elements have been added to PIFAs to improve their operation close to a metal plane [19]. Others have tried to combine techniques to get the desired characteristics. Ukkonen et al. tested a patch antenna operating above a EBG and

obtained a read range of over one meter when the antenna was placed on a ground plane [18].

All the papers cited do propose antennas that will work if they are created and used according to specifications, but the task has yet been accomplished to create an antenna that will operate reliably in a variety of different environments attached to a variety of different objects.

This research begins by taking a necessary step back to see and test exactly what is happening electromagnetically as the antenna approaches the ground plane. With a clear understanding of the physics, the problems can then be addressed.

CHAPTER III

THE PLANAR FOLDED DIPOLE

This study focuses on the characteristics of the planar folded dipole. The planar folded dipole is chosen because of its favorable properties when used in a RFID system. Fabrication of a planar folded dipole antenna is very simple and inexpensive. It can actually be printed on a common PET substrate, often using conductive inks with an ink jet printer. The folded dipole was chosen over the regular dipole because it has better impedance characteristics and similar gain characteristics. Whereas the impedance of a regular dipole is about 75Ω, the impedance of the folded dipole can be adjusted according to how the dipole is designed. The dipoles designed for this study were made by masking a PET substrate and painting the mask with a silver paste. They were designed to have a 233Ω impedance. A milled copper antenna was also created as a baseline. The dimensions were based on [6], and they are given in Figure 9.

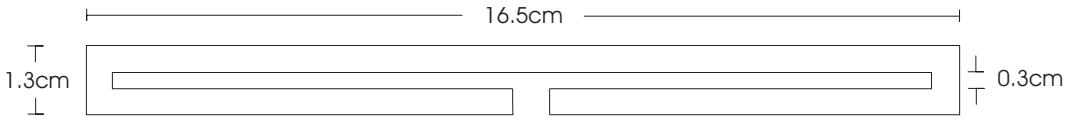

Figure 9: The basic planar folded dipole schematic for 915MHz.

3.1 Simulations

Before the antennas were built and the measurements were taken, simulations were performed using Numerical Electromagnetics Code (NEC). NEC is a method of moments code for modeling antennas. Since NEC performs best when the antennas are modeled as a round wire, the modeled antenna was a line that traversed the center of the planar antenna's dimensions.

A perfectly conducting, infinite ground plane was placed on the $z = 0$ plane, and the antenna was modeled at different heights above the plane. Matlab was used to create the

NEC code for the antenna and step the antenna towards the ground plane. A simulation of the gain patterns of a perfectly matched, 100% efficient antenna as the antenna is moved inside of 0.5λ is given in Figure 10a. The impedance of the same antenna is given in Figure 10b. Within this range, the impedances qualitatively agree with Raumonen et al. in [14]. The gain simulations show that as the antenna gets close to the plane, the signal gets more directive (the blue pattern). It also shows that the antenna's impedance characteristics are extremely varied based on the distance from the ground plane. For the gain pattern, NEC does not take into consideration the impedance mismatch and assumes a system efficiency of 100%. The gain pattern also goes against intuition. Intuitively, the pattern would get less directive because the signal is destructively interfering on the $\hat{z}$ axis; however, these measurements show that the signal is stronger on the $\hat{z}$ axis. This will later be confirmed using experimental data which will show that although the signal does weaken as it is moved close to the plane, it does become more directive.

To study what is happening to an RFID antenna that is tagging a metal object, it is more useful to study the simulations when the antenna is very close to the ground plane. Figure 11 shows the real and imaginary part of the impedances from 0.001λ to 0.06λ. In this region, the real impedance has a parabolic shape. This is very interesting for the design engineer because a small increase in electromagnetic separation distance causes a large increase in impedance. Figure 11 shows that a low impedance is no longer a problem

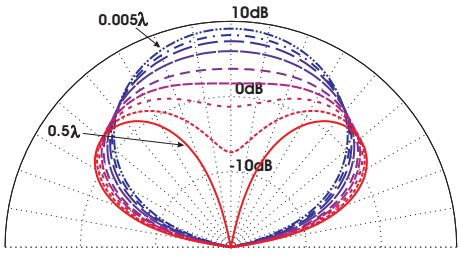

(a) The gain patterns of a 100% efficient folded dipole antenna as it is moved from 0.005λ (blue) to 0.5λ (red).

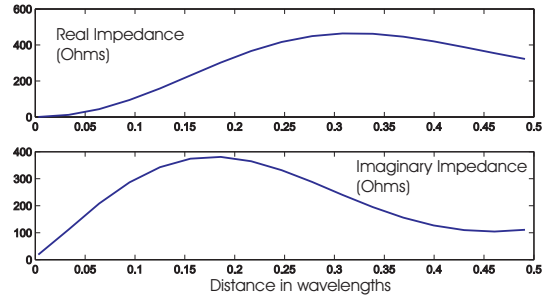

(b) The real and imaginary impedance as the antenna is moved from 0.001λ to 0.05λ.

Figure 10: Gain patterns (a) and impedance simulations (b) as the a folded dipole antenna is moved from 0.001λ to 0.5λ.

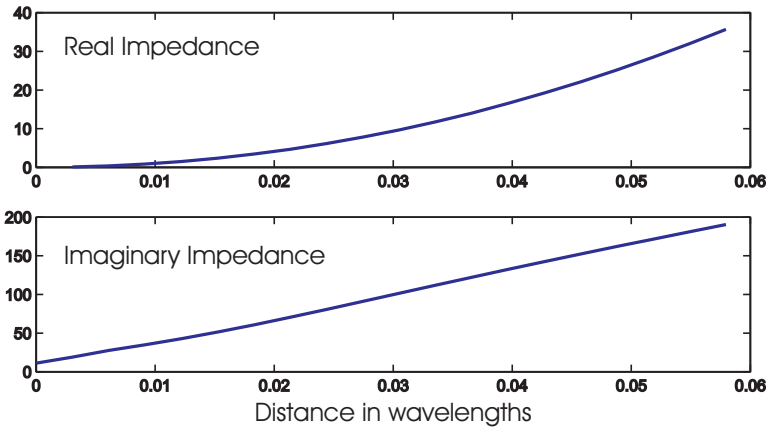

Figure 11: Simulations of the impedance of a half-wave folded dipole approaching a metallic PEC surface inside of 0.06 wavelengths.

when the antenna can be placed at a several hundredths of a wavelength away from the ground plane.

3.2 Experimental Data

3.2.1 Experimental Setup

After the simulations were complete, experiments were conducted to discover what the effect of the metal ground plane would be on the one way link. Figure 12 shows the block diagram with all the components used to measure the impedance of the antenna. All measurements were taken on an outdoor antenna range pictured in Figure 13. This range is on roof of the Van Leer building on the Georgia Tech campus, and it acts as a very good range for these measurements because there are few nearby objects which would cause signal reflections. There is an 8.3 meter separation distance between the two antennas, so the antennas are operating in the far-field.

For the impedance measurements, the network analyzer was set to return the real and imaginary parts of the impedance, and it was calibrated at the end of the transmission line

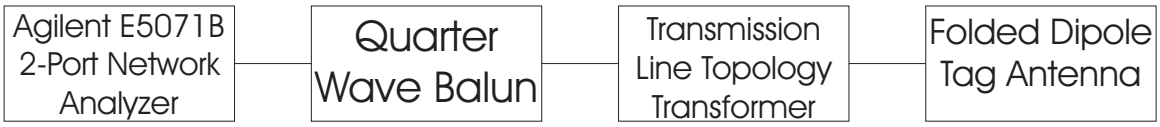

Figure 12: A block diagram of the experimental setup for the impedance measurements.

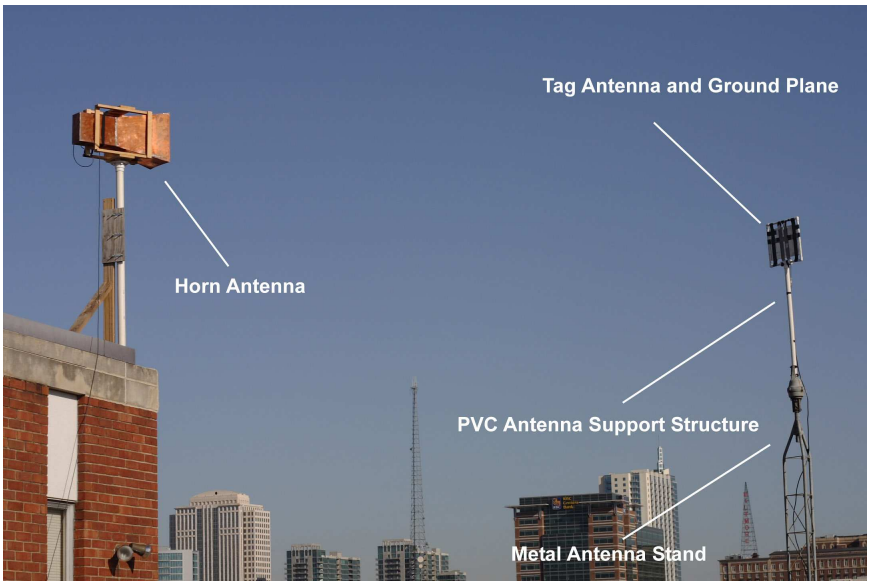

Figure 13: The Van Leer rooftop antenna range.

that connected the network analyzer to the quarter wave balun. This was done to calibrate out any of the effects caused by imperfections in the transmission line. Since the connector to the network analyzer was a 50Ω coaxial cable, effects of the balun and the transmission line topology transformer were calibrated out according to Appendix B, so all impedance measurements include only the antenna. A close-up of the antenna and balun structure is given in Figure 14. The quarter wave balun is used to convert the unbalanced signal from the coaxial cable to the balanced signal needed for the folded dipole to radiate properly. The transmission line topology transformer consists of two copper traces on FR4 board which connect the balun to the antenna.

The impedance was measured for the antenna in free space, then an aluminum ground plane measuring 40cm × 34cm was introduced to the system. Cardboard pieces (assumed to be electromagnetically transparent) were used as spacers between the antenna and the ground plane. Due to the transmission line topology transformer, the antenna could not be brought closer to the ground plane than 0.6cm or 0.02λ. The antenna was then moved from 0.6cm (0.02λ) to over 3cm (0.1λ) in 0.3cm (0.01λ) increments. At each step, the impedance was measured using the network analyzer.

To measure the gain pattern, the antenna was placed on on the PVC support structure

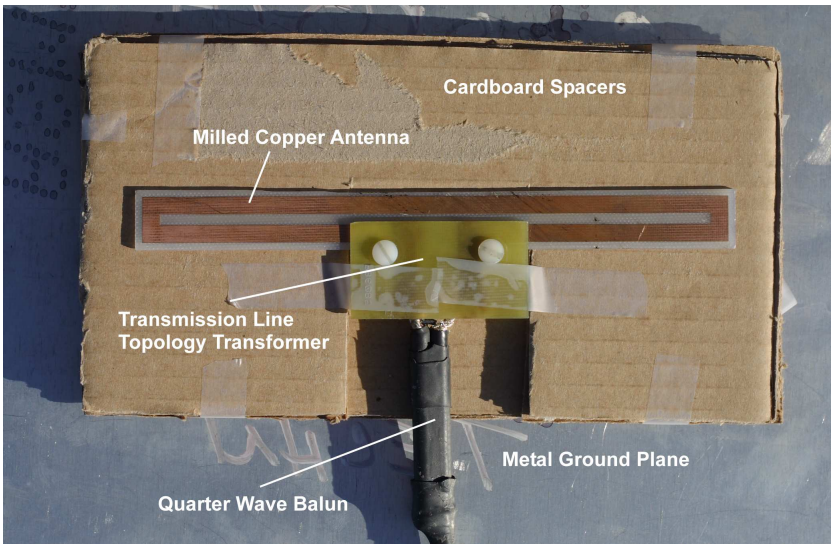

Figure 14: A close-up of the 915MHz half-wave dipole antenna and ground plane.

and rotated 360 degrees. Figure 15 is a block diagram of the experimental system to measure the pattern of the antenna. For these measurements, the balun of the tag antenna was connected to a continuous wave signal generator operating at 915MHz. The horn antenna acts as the receiving antenna, and its received power is filtered and sent to the Agilent E4407B spectrum analyzer which is interfaced with the computer through Matlab. In an actual RFID system, the tag antenna would be the receiver and the horn would be the transmitter, but due to antenna reciprocity [15], the measurements can be conducted with either setup and the same results will be obtained.

This setup conforms to [5] with the exception of the tunable impedance transformation

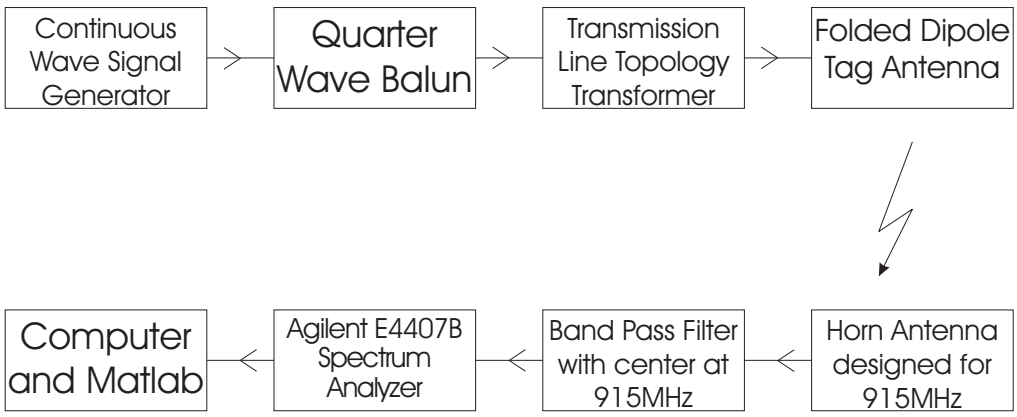

Figure 15: A block diagram of the experimental setup for pattern measurements.

network, but the purpose of the tunable impedance transformation network is to match the unknown impedance of the antenna to the impedance of the transmission line. Since the impedance was measured before the pattern measurement was taken, the impedance mismatch was mathematically calculated out of the gain pattern measurement using equation (18).

$$\Gamma = \frac{Z_a - Z_l}{Z_a + Z_l} \tag{18}$$

In the calculation, $(1 - \Gamma)$ is the fraction of voltage transferred to the antenna, Z_a is the measured impedance of the antenna, and Z_l is the impedance of the transmission line (50Ω). For example, if Γ is calculated from the measured impedance of the antenna to be 0.5, then the received power of the antenna is 50% lower than it would be if there was a perfect match; therefore, 50% of the received power is added to the gain pattern.

In order to get meaningful measurements in any experimental setup, careful attention must be paid to calibration of the system. For the transmitting system, all of the feeding transmission lines were connected together just as they were in the experiment and the loss across those lines was measured. For the receiving system, all the cables and the band pass filter were connected exactly as they were in the experiment and then the loss was measured; therefore, the characteristics of the transmitting RFID antenna, the receiving horn antenna, the balun, and the transmission line topology transformer were measured in these experiments. Along with these calibrations considerations, most of the interesting data here are the patterns relative to the free space pattern, so measurements were taken without the ground plane present. These measurements can be reasonably approximated as free space measurements because there are no electromagnetically significant objects within several wavelengths of the antenna. All patterns that included the ground plane, were normalized to the maximum power received when the antenna was measured in free space.

3.2.2 Results

Figure 16 shows the gain patterns of the milled copper antenna (a) and the antenna made from silver paste painted on a PET substrate (b). Both are normalized to the maximum received power when the copper antenna was transmitting. As expected, these patterns are

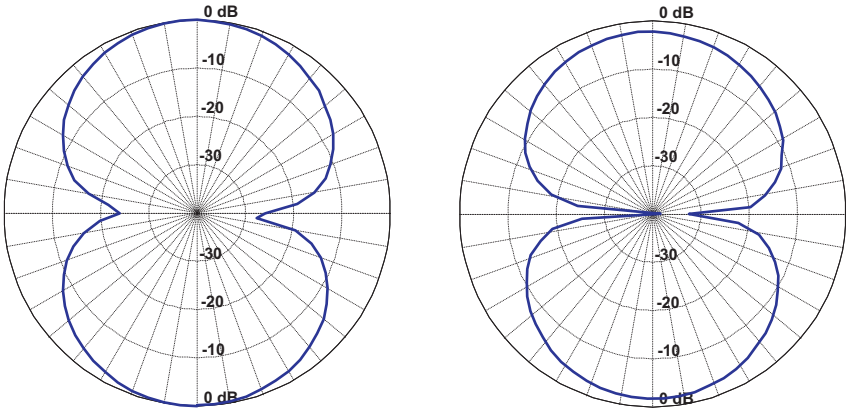

(a) The measured gain pattern of the copper antenna.

(b) The measured gain pattern of the silver paste antenna.

Figure 16: The measured gain pattern for the milled copper and the silver paste half wave dipole antennas for 915MHz, normalized to the copper antenna.

very similar; the main difference is that there is about 2dB less received power when the silver paste antenna is transmitting. This shows that the flexible, silver paste antenna has characteristics very similar to the rigid milled copper baseline.

To study the affect antenna trace width had on the design, a third antenna was fabricated. This antenna was also made by masking a PET substrate and painting a silver paste on the mask; however, the trace width is half as wide as the other antennas. Figure 17 shows the antenna structure (a) and its pattern in free space normalized to the copper, full width antenna (b). The pattern is similar to the thick copper antenna, but its pattern is about 6dB lower than the copper trace width.

Figure 18 shows three patterns measured for the copper, silver and thin antennas. All plots on this figure are normalized to the free space copper antenna. This figure is provided to show the range of penalty due to the ground plane for each antenna. Notice for the case where the antenna is 0.1λ away from the ground plane, its directivity gives the antenna additional gain instead of penalizing the gain.

In Figure 18a and Figure 18b we again see the antennas are very similar in performance; however, the thin antenna suffers from a much greater penalty due to the ground plane. Combined with the fact that the thin antenna does not radiate well in free space, these results make the thin antenna a poor choice if the only factor is power pattern.

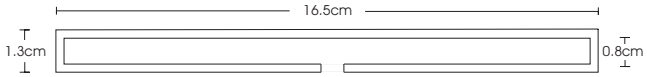

(a) The dimensions of the thin antenna.

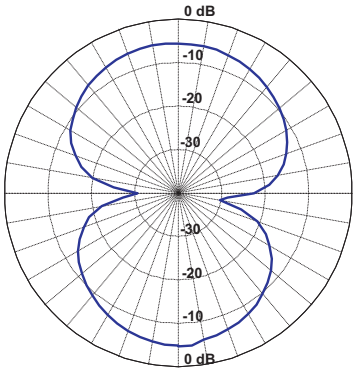

(b) The free space gain pattern of the thin antenna.

Figure 17: The thin antenna was created to study the effect of trace width. The gain pattern is normalized to the standard width, milled copper antenna.

Table 1 shows the gain penalty versus distance for all three antennas. Note the sign change for the relative gain of the antenna as the added directivity begins to overcome the losses due to destructive interference.

Table 1: Gain penalty due to ground plane (dB)

Distance (cm)	Copper	Silver	Thin
0.6	-4.7	-4.2	-8.6
0.9	-3.0	-2.4	-5.5
1.3	-1.2	-1.2	-4.1
1.6	-0.3	-0.5	-2.1
2.0	0.4	-0.1	-1.1
2.3	1.1	0.6	-0.9
2.6	1.5	1.1	0.1
2.9	1.9	1.5	0.7

3.3 Impedance Measurements

The impedance measurements for these antennas are also very important to this study. Figure 19 show the measurements for the copper (a) and the silver (b) antennas. Qualitatively, these results match the simulations; however, quantitatively, the measured results are more encouraging. Recall that the main problem is the antenna impedance approaching zero as the antenna approaches the ground plane. Figure 19 shows that the impedance of the antennas coupled with the balun is significantly higher compared to the simulations (Figure

10b) at the same electromagnetic distance. This could be due to a number of factors including the simulations were done with an ideal ground plane and antenna, a wire antenna instead of a planar antenna, and an infinite ground plane. The simulations performed in this study were designed to give a general, theoretical background in order to measure the validity of the experiments. Therefore, where the experiments and the simulations differ, the experiments can be considered to be more accurate than the simulations.

A likely cause for the mismatch between the simulations and the measurements also includes the DC resistance of the fabricated antennas. Since the antennas being measured are folded dipoles, the DC resistance is an important factor. The current getting burned up due to the DC resistance will change radiation properties of the antenna, causing the antenna to have a more favorable input impedance.

Note that the real impedance for the copper antenna is around 12Ω even at the lowest measuring distance of 0.02λ. This is encouraging considering the simulations put this number at nearly zero.

Interesting in Figure 19b is that the real impedance is higher for the silver than the copper (Figure 19a). This is probably due to the fact that the silver antenna has a greater DC resistance than the copper does. At around 20Ω for a separation distance of 0.02λ, this impedance very close to the ground plane might be high enough to be used in a modulated backscatter system. Keep in mind at the testing frequency of 915MHz (a common frequency in the ISM band used for RFID), 0.02λ is about 0.6cm. For many applications, a 0.6cm tag-object separation distance is still considered to be too large.

Impedance measurements were also taken for the thin folded dipole given in Figure 17a. Shown in Figure 20, these measurements are quite interesting in that the real impedance of the thin antenna is largely unaffected by the proximity to the ground plane. It even appears to perform better when close to the metal object. Before one gets too excited about the favorable impedance characteristics, remember the unfavorable gain characteristics. The gains presented for these experiments assume a perfect match between the antenna and the feed structure, but recall in free space, the received power for the thin antenna was about 6dB less than the copper and 4dB less than the silver paste (Figure 17b). When attached

to metal, the thin antenna's gain penalty for 0.02λ separation distance was 8.6dB compared to 4.7dB for copper and 4.2dB for the silver paste (Table 1).

The significant differences shown here can possibly be explained by the antenna's DC properties. Before any experiments were conducted, all three of the antennas' DC resistances were measured. As expected, the copper antenna had very little DC resistance, and silver paste antenna's DC resistance was about 10Ω. The thin silver antenna, however, had a much higher DC resistance – on the order of $1k\Omega$. Therefore, much of the power sent to the thin antenna was not begin radiated at all, but rather was being consumed in Ohmic losses. Because of this, the thin antenna was probably not performing as a folded dipole but was rather radiating only in the small region close to the feed where the power had not yet been consumed by the Ohmic losses.

The high ohmic losses in the thin antenna introduce a trade-off in the design of RFID antennas. A folded dipole antenna can be fabricated to have favorable impedance characteristics, but as demonstrated here, the favorable impedance characteristics are at the expense of favorable radiation characteristics. Research could be done to explore the best impedance-radiation trade off in antenna design, and antenna thickness and DC resistance should be considered major components on that research.

Which of the studied antennas is the best for an RFID tag on a variety of objects, including metal? Although that is a subjective question, of these three, the silver paste antenna of standard size is the best. The silver paste antenna had a slightly smaller gain penalty due to the ground plane than the copper did. It also had a substantially better impedance than the copper antenna at the same electromagnetic distance. The silver paste antenna was also inexpensive and easy to fabricate, and it is flexible. Since the free space gain was only 2dB less than the copper antenna, this antenna stands out as the best performer in these experiments.

These experiments, however, did not measure the antenna any closer than 0.02λ, and as mentioned above, this is simply not acceptable if RFID is to move from the current, limited application to a broader use in a variety of markets. The question becomes: "Can these antennas be moved any closer to the plane and still operate?"

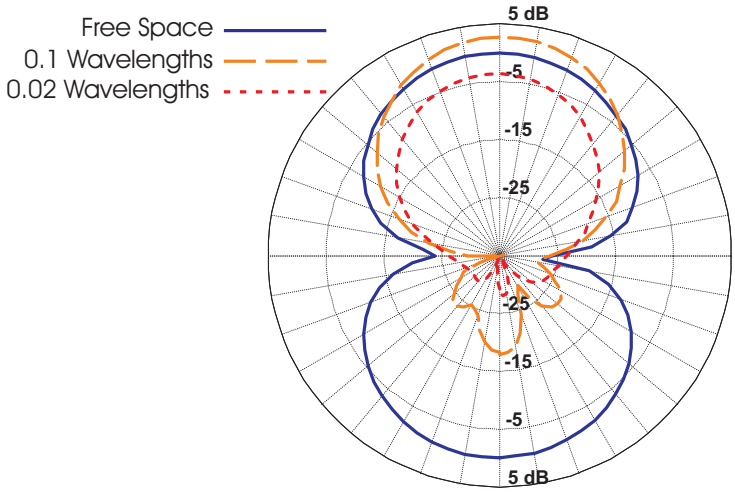

(a) Milled copper.

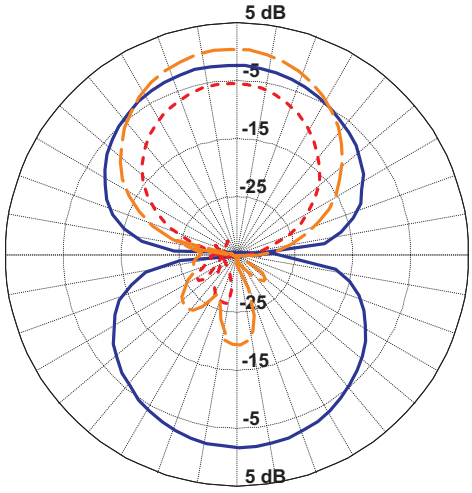

(b) Silver paste.

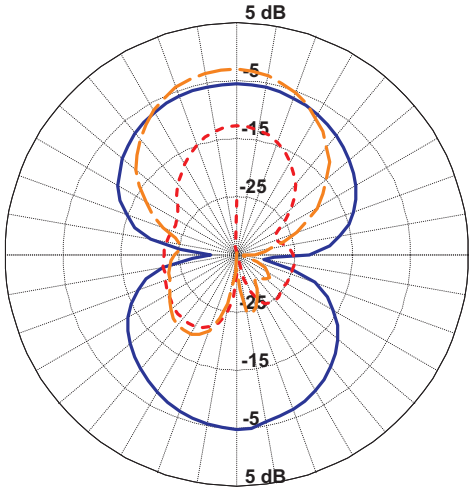

(c) Thin design.

Figure 18: Power range plots show the effect of the ground plane on antennas' gain pattern. For the case when the antenna was closest to the ground plane, the gain was lower than the free space gain. For the case when the antenna was further from the ground plane, the increased directivity caused the gain to be higher than the free space gain.

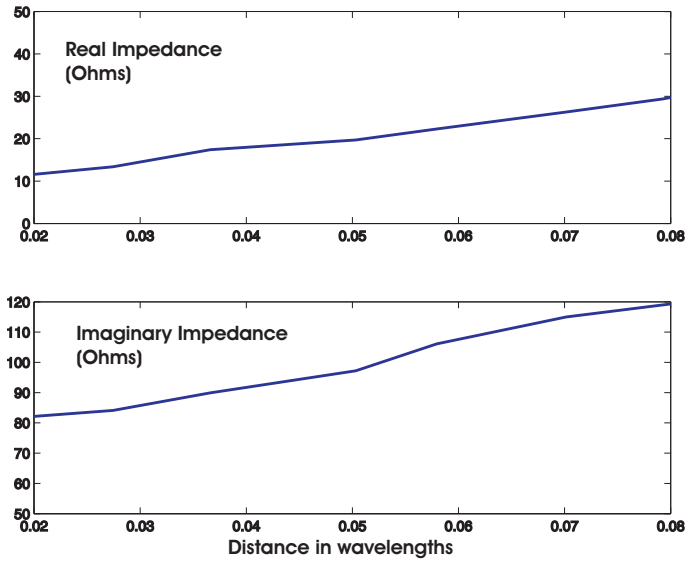

(a) Copper Antenna.

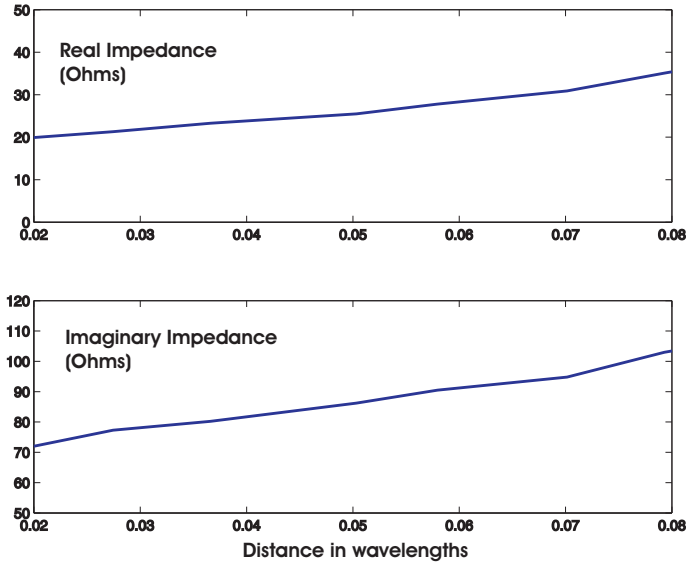

(b) Silver Antenna.

Figure 19: The real and imaginary impedance of the 915MHz planar, half wave dipole antennas show better results than the simulations.

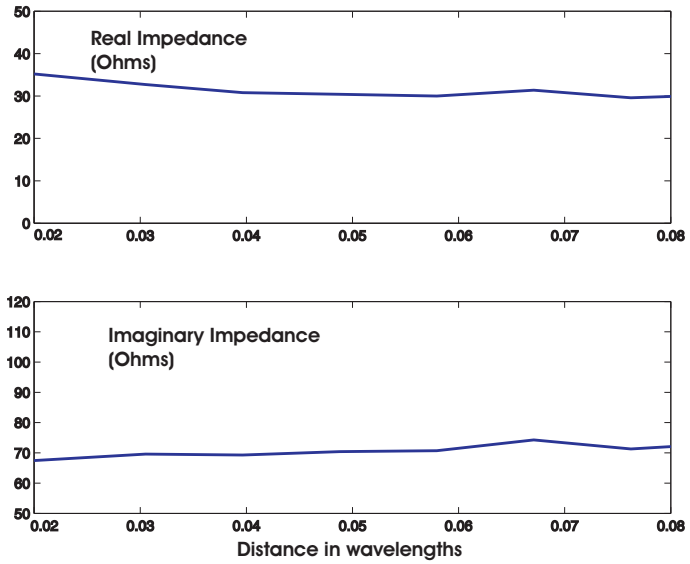

Figure 20: The impedance of the thin antenna is largely unaffected by the proximity of the ground plane.

CHAPTER IV

A DIELECTRIC BARRIER

This chapter will present theory and experiments which demonstrate a way to move an antenna physically close to a ground plane while keeping a large electromagnetic distance. Although physical distance and electromagnetic distance have been considered directly proportional to this point, they do not have to be considered as such. There are three basic ways to change electromagnetic distance. The first and least interesting to this study is to increase physical distance; however, non-trivial height is to be avoided for the RFID tag. A second way to increase electromagnetic distance is to increase operating frequency. The experiments in the previous chapter were conducted at 915MHz, making 6mm about 0.02λ, so if the frequency was doubled 0.02λ becomes 3mm. This presents a strong case for increasing the frequency for normal RFID applications to a higher operating frequency in the ISM band such as 2.4GHz or 5.4GHz; however, as the frequency gets higher, the electronics required to build the tags and the readers become more expensive. The higher frequencies also have higher path and penetration losses.

A third way to increase the electromagnetic distance is to place a dielectric between the antenna and the ground plane. Recall the wavelength of an electromagnetic wave is not constant in all materials, but rather is described by (19).

$$\lambda = \frac{\lambda_{freespace}}{\sqrt{\mu_r \epsilon_r}} \tag{19}$$

Where μ_r is the relative permeability of the material, and ϵ_r is the relative permittivity. If the electromagnetic wave between the antenna and the ground plane could travel through a dielectric with a high ϵ_r, then the wavelength between the antenna and the ground plane would be much shorter, effectively changing the electromagnetic distance between the ground plane and the antenna (see Figure 21). For example, consider the measurements

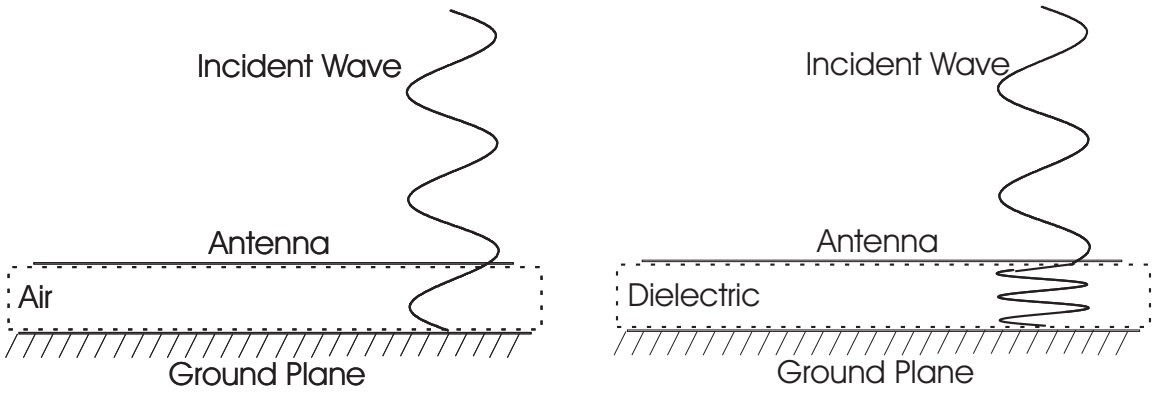

Figure 21: When a dielectric spacer is used, physical distance is the same, but the electromagnetic distance is increased (right).

taken in Chapter 3. If the 0.02λ separation distance was filled with a dielectric of permittivity 25, then the effective increase in electromagnetic distance would be $\sqrt{25} = 5$, so now the antenna is separated from the ground plane by 0.1λ. As shown in previous experiments, the antenna can function quite well from that distance.

Since the desire in most RFID applications is to have a trivial width of the antenna, the dielectric used would need to have a very high permittivity so it could maximally decrease the wavelength while minimally increasing the distance.

One familiar with the interaction between electromagnetic waves and dielectric materials knows that the problem is not as simple as just creating a very high dielectric constant material. An electromagnetic wave does not only reflect off a metal ground plane, but some of the power also reflects off the dielectric. As the dielectric constant gets larger, the portion of reflected power also gets larger.

For normal incidence, the plane wave encountering a dielectric can be analyzed like a wave on a transmission line encountering a load, so the reflection coefficient equation for a transmission line, equation (20), becomes the reflection coefficient equation for a normal incident plane wave, equation (21).

$$\Gamma = \frac{Z_l - Z_t}{Z_l + Z_t} \tag{20}$$

In equation (20), Z_l is the impedance of the load, and Z_t is the impedance of the transmission line. For the normal incident plane wave, Z_l maps to η_d, the characteristic impedance of

the dielectric medium, and Z_t maps to η_f, the characteristic impedance of air.

$$\Gamma = \frac{\eta_d - \eta_f}{\eta_d + \eta_f} \tag{21}$$

The intrinsic impedance of a medium, η is the material's permeability over its permittivity, given in equation (22).

$$\eta = \sqrt{\frac{\mu}{\epsilon}} = \sqrt{\frac{\mu_o \mu_r}{\epsilon_o \epsilon_r}} \tag{22}$$

Where μ_o and ϵ_o are constants describing the permeability and permittivity of free space, and μ_r and ϵ_r are the relative permeability and permittivity for a material. For air, $\mu_r = 1$ and $\epsilon_r = 1$, but for a dielectric material μ_r and ϵ_r can be greater than 1. Most materials used in electronics are non-magnetic, so μ_r is often considered to be 1. Substituting (22) into (21) gives (23).

$$\Gamma = \frac{\sqrt{\frac{\mu_o \mu_{r,die}}{\epsilon_o \epsilon_{r,die}}} - \sqrt{\frac{\mu_o \mu_{r,air}}{\epsilon_o \epsilon_{r,air}}}}{\sqrt{\frac{\mu_o \mu_{r,die}}{\epsilon_o \epsilon_{r,die}}} + \sqrt{\frac{\mu_o \mu_{r,air}}{\epsilon_o \epsilon_{r,air}}}} \tag{23}$$

Assuming $\mu_r = 1$ (23) becomes (24).

$$\Gamma = \sqrt{\frac{\mu_o}{\epsilon_o}} \left(\frac{\frac{1}{\epsilon_{r,die}} - 1}{\frac{1}{\epsilon_{r,die}} + 1} \right) \tag{24}$$

From (24) it can be seen that increasing the relative permittivity of the dielectric causes the reflection coefficient to move from its ideal value of 0.

4.1 Experimental Design

In order to test the theory of a dielectric buffer, experiments were designed and conducted where the impedance and power pattern of folded dipole antennas were measured when a dielectric buffer was placed between the antenna and the ground plane. The same setup and equipment given in Chapter 3 was used in these measurements with one notable exception. All the dipoles measured in these experiments were milled copper on FR4 dielectric, so the transmission line topology transformer was not used. The balun was soldered directly to the copper of the antenna. Given in Figure 22, the antennas were designed with a variety of trace widths and top–bottom separation distances, therefore, these experiments not only

measured the effect of the dielectric buffer, but they also measured the effect of antenna design.

Each antenna was placed as close as possible to the ground plane then stepped back in 0.3cm increments. At each position, the impedance and pattern were measured according to the procedure described in Chapter 3. Since the transmission line topology transformer was not used in these measurements, the antenna could be placed much closer to the ground plane. The FR4 board was actually placed directly on the ground plane. At each height above the ground plane, the antenna was measured with the cardboard spacer and with a dielectric spacer composed 1.5mm dielectric slabs with increasing ϵ_r moving from the antenna to the ground plane. For example, if the antenna was 0.3cm away from the ground plane, two dielectric slabs were used. The one close to the antenna had an ϵ_r equal to 2, and the one closest to the ground plane had an ϵ_r equal to 3. When the antenna was furthest away from the ground plane (0.9cm), the dielectric slabs had a dielectric constant from 2 to 10. This "graduated dielectric" idea was introduced in order to minimize reflections at the dielectric surface.

These measurements will not only give insight into the effect of the dielectric spacer, but they will also allow a comparison to be made between the different antenna geometries.

4.2 Experimental Results

Since the results of these experiments compare the performance of the dielectric spacer and antenna design, they will be presented in two sections. One section will compare antenna performance with and without the dielectric, and one will compare the antenna designs. All measurements can be found in Appendix A.

4.2.1 Dielectric Spacer Effects

The purpose of placing the dielectric spacer between the antenna and the ground plane was to electromagnetically move the antenna away from the ground plane without changing the physical distance or the frequency of operation; however, as shown at the beginning of the chapter, electromagnetic waves reflect off the high dielectric much the same way they reflect

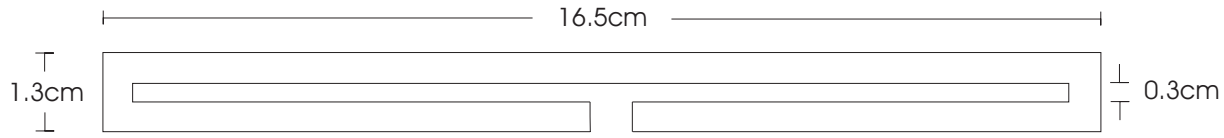

(a) Standard dimension.

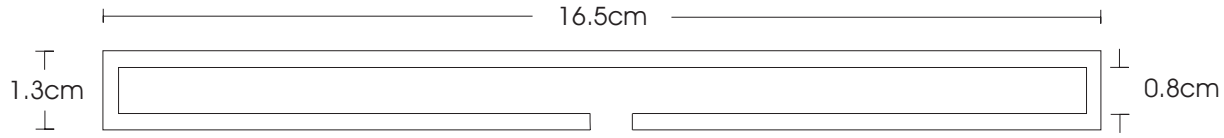

(b) Medium trace width, wide separation distance.

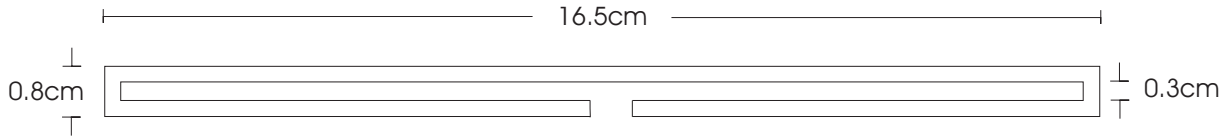

(c) Medium trace width, medium separation distance.

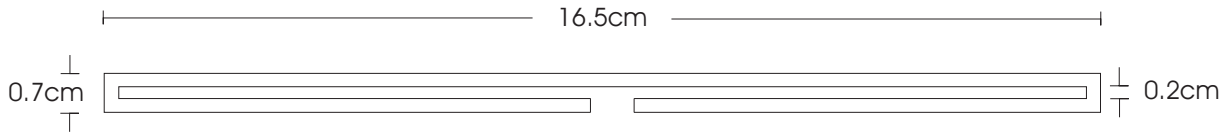

(d) Medium trace width, narrow separation distance.

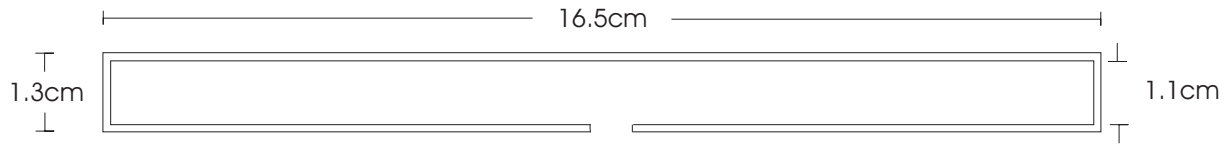

(e) Thin trace width, large separation distance.

Figure 22: The different designs of the 915MHz planar, half wave dipole antennas used in the study of the dielectric. All antennas are made of milled copper on a FR4 substrate.

off the ground plane. These experiments were conducted to see if the dielectric barrier would enhance the performance of the antenna compared to the case when the dielectric barrier was not present. The results below show the patterns for the case where the antenna in free space as well as when the antenna was 0.3cm above the ground plane. For the 0.3cm case, the pattern is shown with and without the dielectric spacer. All patterns are normalized to the case where the antenna is in free space. Figure 23 shows the patterns and Table 2 shows the impedance measurements.

The pattern measurements in Figure 23 clearly show that the dielectric spacer greatly hinders the ability of the antenna to radiate efficiently. The dielectric causes about 10dB of loss compared to the case where there is no dielectric buffer. Adding this loss to the loss due to the ground plane, the antenna now has over 20dB of loss in the forward link compared to the free space measurement. Recall that the loss in the backscatter link is twice the forward link, causing the ground plane and dielectric spacer penalty to be over 40dB. Obviously, this is unacceptable in an RFID link for both power-up and modulation.

Table 2 shows the impedance measurements for all the antennas. Without the dielectric, they all have very similar impedances with the real part being around 88Ω. As expected the impedance generally does increase as the antenna moves away from the ground plane, but the increase is very small. Since these measurements are taken very close to the ground plane and each step is only 0.01λ, the small increase is not surprising. For all antennas, the presence of the dielectric spacer greatly decreases the impedance. The impedances marked with asterisks can be considered as zero. The dielectric did not increase the impedance as expected. This might be due to the fact that the dielectric constant is "graduated" rather than constant throughout, creating more interfaces and reflections than would be present with a simple dielectric in place.

Since these graduated dielectrics did not improve the impedance and caused the extremely large negative effect on the power output, this "graduate dielectric" is a poor idea for RFID technology. These measurements do however, invite the question: "Can a buffer be created that will increase the impedance while not decreasing the power being radiated?"

In exploring this question, the first step would be to try to discover what is causing the

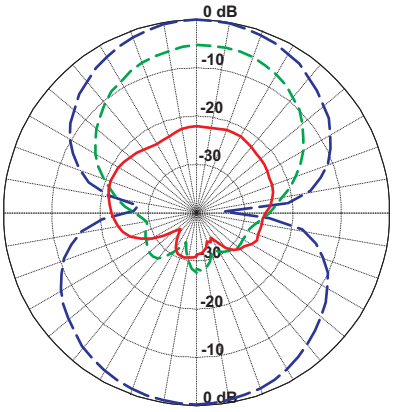

(a) The standard width antenna.

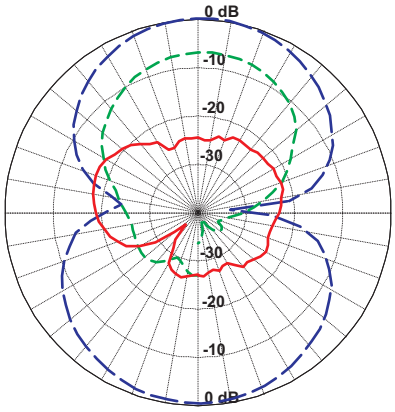

(b) The medium trace width, wide separation distance antenna.

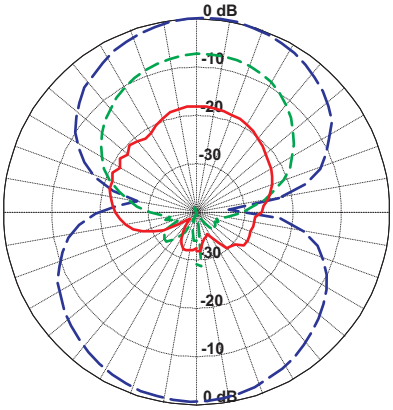

(c) The medium trace width, medium separation distance antenna.

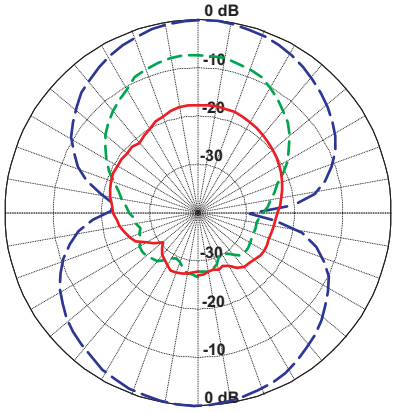

(d) The medium trace width, small separation distance antenna.

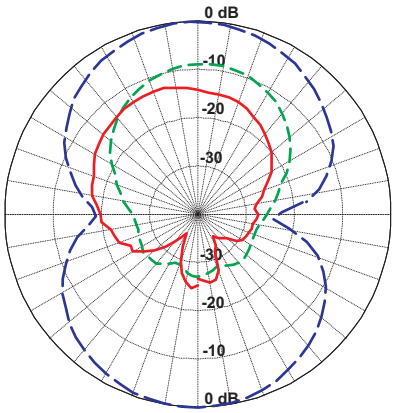

(e) The thin trace width antenna.

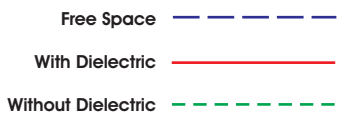

(f) Pattern legend.

Figure 23: The effect of the dielectric substrate on the 915MHz planar, folded dipole antennas. Each figure shows the measurement in free space (blue), 0.3cm away from the ground plane without the dielectric (green), and 0.3cm away from the ground plane with the dielectric (red).

Table 2: Impedance measurements with and without the dielectric spacer

Distance (λ)	Impedance (Ω) without dielectric	Impedance (Ω) with dielectric
0.01	84.1 + 31.1j	40.0 - 8.8j
0.02	88.7 - 44.0j	16.4 - 15.6j
0.03	89.0 - 49.8j	*-9.4 - 55.2j

(a) Impedance measurements with standard trace width antenna

Distance (λ)	Impedance (Ω) without dielectric	Impedance (Ω) with dielectric
0.01	86.8 - 34.2j	35.2 - 10.0j
0.02	88.8 - 39.5j	1.39 - 29.8j
0.03	89.3 - 41.5j	9.3 - 102j

(b) Impedance measurements with medium trace width, wide separation distance

Distance (λ)	Impedance (Ω) without dielectric	Impedance (Ω) with dielectric
0.01	83.3 - 30.3j	23.6 - 13.1j
0.02	91.4 - 50.0j	*-6.9 - 53.2j
0.03	86.1 - 36.9j	67.3 - 106j

(c) Impedance measurements with medium trace width, medium separation distance

Distance (λ)	Impedance (Ω) without dielectric	Impedance (Ω) with dielectric
0.01	89.5 - 49.3j	18.6 - 15.4j
0.02	89.5 - 58j	*-2.1 - 34.4j
0.03	87.3 - 69.3j	8.6 - 97.1j

(d) Impedance measurements with medium trace width, small separation distance

Distance (λ)	Impedance (Ω) without dielectric	Impedance (Ω) with dielectric
0.01	89.8 - 47.6j	*-4.3 - 46.2j
0.02	90.2 - 50.6j	0.7 - 87.9j
0.03	90.4 - 56.0j	55.2 - 11.2j

(e) Impedance measurements with small trace width, large separation distance

loss of radiated power. Figure 24 shows the patterns of the antenna when the FR4 it is milled on is placed directly on the ground plane (blue, dashed line) and when the FR4 is 0.3cm away from the ground plane with the dielectric spacer between the ground plane and the antenna (red, solid line). The antenna used for this comparison is the standard width antenna.

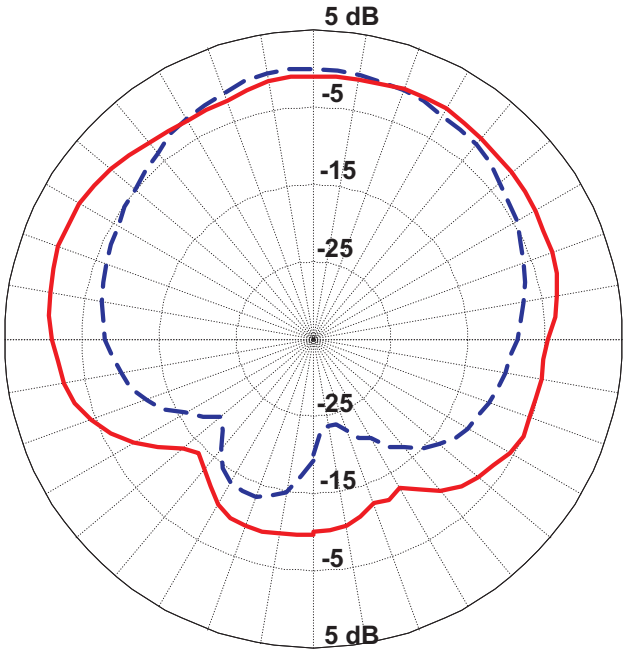

Figure 24: The patterns when the FR4 the antenna is milled on is placed directly on the ground plane (blue, dashed line), and when the FR4 the antenna is milled on is placed directly on the dielectric spacer (red, solid line).

The two patterns are very similar suggesting that the reflections taking place at the dielectric buffer interface are very similar to the reflections taking place at the ground plane. How can the reflections be minimized? The reflections can be minimized by using magnetic materials.

4.2.2 Magnetic Buffer Material

In equations (22) through (24), μ_r was always considered to be one because most materials are non-magnetic, and electromagnetic engineers usually make this assumption to in order to simplify design; however, in this case, increasing the the permeability along with permittivity so the ratio of the permeability to permittivity (μ/ϵ) remains constant could

be the key to creating a buffer that increases the electromagnetic distance and, therefore, the impedance while not decreasing the power radiated. Recall from equation (22) that the intrinsic impedance of a material is equal to the square root of the permeability over the permittivity.

$$\eta = \sqrt{\frac{\mu}{\epsilon}} = \sqrt{\frac{\mu_o \mu_r}{\epsilon_o \epsilon_r}} \tag{22}$$

So if a material could be made that had a high permittivity, a high permeability, and the ratio of the two match the ratio of air, then the incoming signal would not be reflected at the air – dielectric interface because equation (23) would equal zero.

$$\Gamma = \frac{\sqrt{\frac{\mu_o \mu_{r,die}}{\epsilon_o \epsilon_{r,die}}} - \sqrt{\frac{\mu_o \mu_{r,air}}{\epsilon_o \epsilon_{r,air}}}}{\sqrt{\frac{\mu_o \mu_{r,die}}{\epsilon_o \epsilon_{r,die}}} + \sqrt{\frac{\mu_o \mu_{r,air}}{\epsilon_o \epsilon_{r,air}}}} \tag{23}$$

All of the incoming signal would be coupled into the dielectric and would have a wavelength described by equation (19).

$$\lambda = \frac{\lambda_{freespace}}{\sqrt{\mu_r \epsilon_r}} \tag{19}$$

This would allow the needed increase in electromagnetic distance while not creating a reflective interface causing destructive interference.

4.2.3 Antenna Design Effects

The experiments conducted not only give insight into the effect of the dielectric spacer, but they can also give insight into the how antenna design affects the performance of the antenna in the presence of a metal ground plane. The following results will explore how the different designs performed relative to one another. All antennas were normalized to the standard design given in Figure 22a.

Figure 25 compares the different antennas' free space radiation. This figure is presented to show that the characteristics of all five antennas are very similar – varying by no more than about 2dB from the best performer to the worst performer. Since the free space characteristics are similar, no single antenna stands above the rest with regard to free space, so the the focus can be turned to the characteristics when the ground plane is present. Figure 26a shows the different antennas' gain pattern when the antenna is placed at 0.3cm (0.01λ), and Figure 26b is the same for 0.6cm (0.02λ). Both cases do not include

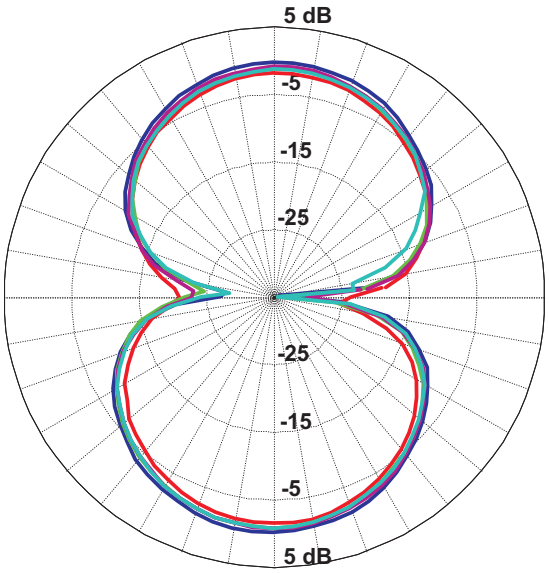

Figure 25: The gain patterns of the five 915MHz planar, half wave dipole antennas in free space show that all have very similar free space performance.

the dielectric spacer. All patterns are normalized to the standard width antenna. Here an

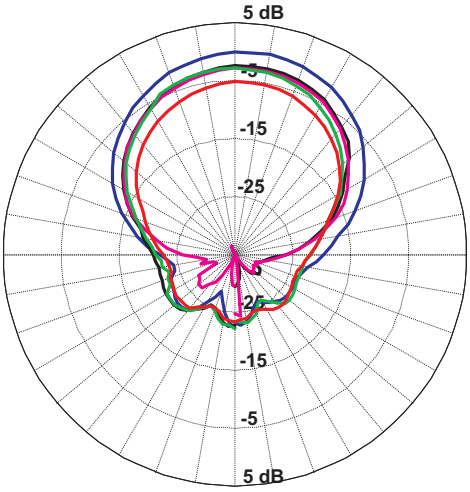

(a) Gain patterns of the five designs 0.3cm away from the ground plane.

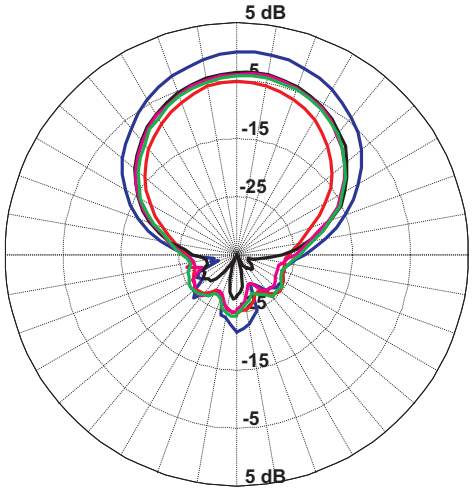

(b) Gain patterns of the five designs 0.6cm away from the ground plane.

Figure 26: Gain patterns of five of the 915MHz planar, half wave dipole antennas when placed 0.3cm (left) and 0.6cm (right) away from the ground plane show that antenna trace width affects gain pattern more than the top–bottom separation distance.

appreciable difference between the best performer and worst performer begins to show. In both cases, the standard antenna (blue) performs about 5dB better than the thin antenna (red). The medium width antennas are bunched together between the standard and the

thin. These results suggest that the trace width affects the radiation more than the top – bottom separation distance in a planar, folded dipole antenna. Since the ground plane has the least influence on the standard width antenna, it emerges as the best among these choices for a RFID chip antenna.

4.3 Conclusion

These experiments were motivated by an idea to electromagnetically move the antenna away from the ground plane by placing a dielectric spacer between antenna and the ground plane. They were also designed to explore the effect of antenna design on radiation characteristics.

As a whole, the dielectric spacer proved to be hinderance to proper antenna radiation; however, the dielectric spacer did improve the impedance of the antennas. With that in mind, it was suggested that a spacer be made with both a high permittivity and high permeability. This would allow the impedance to increase without a decrease in radiation efficiency.

CHAPTER V

CONCLUSION AND CONTINUING RESEARCH

5.1 Conclusion

The problem explored in this work is a basic problem limiting widespread RFID implementation: tag performance degradation when the tag is placed on a metallic object. If these performance degradations could be overcome, RFID would be a reliable identification system suitable for a variety of different environments; however, if these limitations remain, RFID will only find limited usage in specific environments.

The simulations where the impedance and gain pattern were studied versus distance from the ground plane showed that the folded dipole antenna is a good choice for the RFID antenna if it can be placed several hundredths of a wavelength away from the ground plane. Experiments building on the simulations showed that the folded dipole antennas performed better than the simulations predicted, and that the antenna only needed to be moved a few hundredths of a wavelength away from the ground plane, however; in most RFID systems, a few hundredths of a wavelength is too much as it limits the "peel and stick" design requirement for RFID antennas.

To further study how the degradations might be overcome, further experiments were designed and conducted testing the effect of antenna design on the degradation parameters. The experiments conducted showed that antenna trace width affected radiation characteristics more than the separation distance between the top and bottom arms of the folded dipole.

Also explored was the effect of placing dielectric buffer between the ground plane and the antenna. Since the wavelength of a signal in a dielectric is smaller than the wavelength of a signal in air, inserting a dielectric electromagnetically moves the antenna away from the ground plane. The experiments showed that although the antennas' radiation characteristics were severely hindered, the input impedance of the antenna was boosted to a usable level

due to the insertion of the dielectric.

It was theorized that the cause of the radiation hinderance in the presence of the dielectric is due to reflections off the dielectric – air interface. A proposal was made to increase the permeability along with the permittivity of the dielectric in order to remove these reflections.

5.2 Continuing Research

This work is best continued by exploring two areas of interest in reducing the performance degradations: antenna design and the dielectric substrate.

5.2.1 Antenna Design

Only a limited number of trace width and separation distances were explored in this study. Simulations and experiments should be done to find a direct relationship between design parameters (trace width, top – bottom separation distance, and shape) and the performance when the antenna is close to the ground plane.

5.2.2 Dielectric Substrate

An antenna with a high relative permittivity and an equally high relative permeability dielectric buffer should be measured. Since the relative permeability and permittivity are the same, no reflections will take place at the dielectric–air interface, there will be no destructive interference to hinder the radiation, but the impedance will be improved because the antenna will be electromagnetically further from the ground plane than if the there were no buffer. If the permeability and permittivity could be very high, this would allow for a trivial width, very versatile RFID tag antenna that would operate reliably without regard to material attachment.

5.2.3 Multidisciplinary Research

Antenna design and measurement is something that an RF engineer will be very familiar and comfortable doing, but this study requires that research in connection with material design. To find the best system possible, the antenna and the dielectric need to be optimized

for use with each other. This will require collaborative research between material scientists and RF engineers. If this collaborative research can take place, this problem will be solved, and RFID can begin to reach the potential many engineers feel it has.

APPENDIX A

DIELECTRIC EXPERIMENT RESULTS

A.1 Standard Milled Copper Design

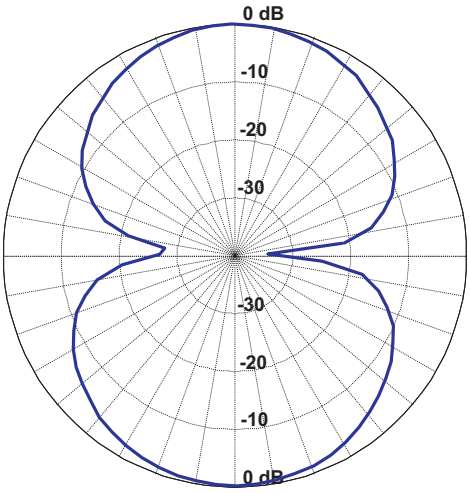

(a) Free space.

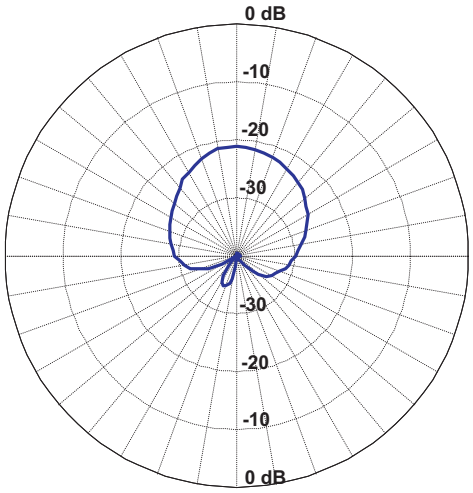

(b) FR4 directly on ground plane.

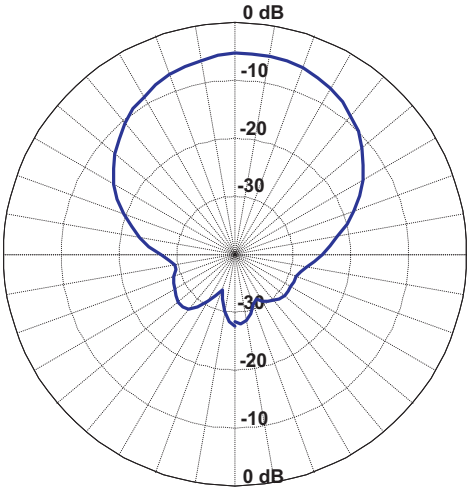

(c) 3mm separation distance, no dielectric

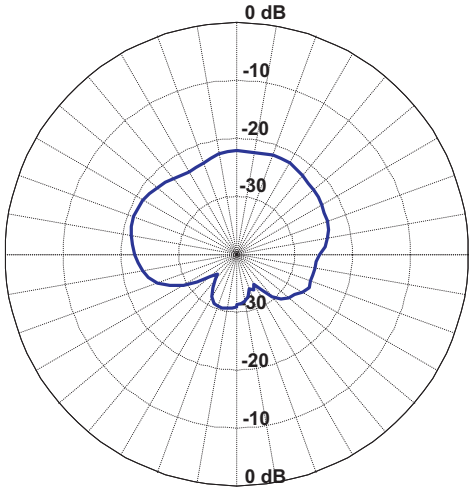

(d) 3mm separation distance, with dielectric

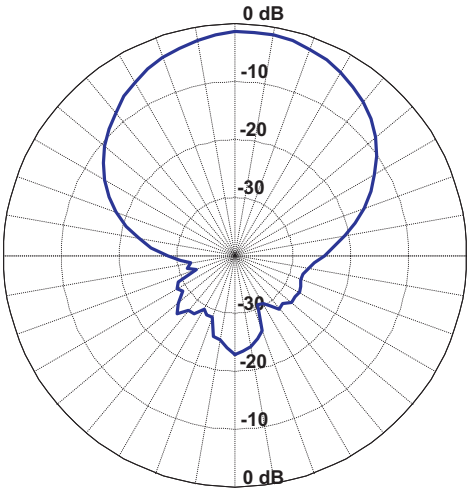

(a) 6mm separation distance, no dielectric

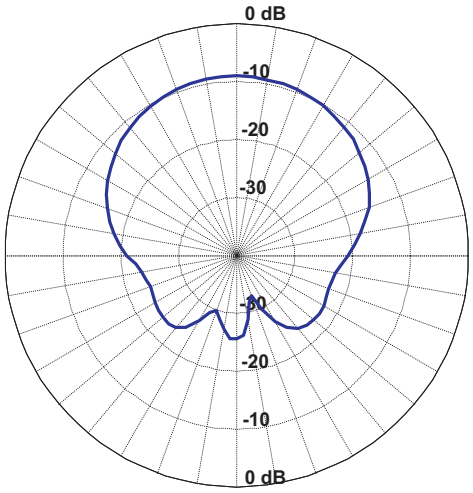

(b) 6mm separation distance, with dielectric

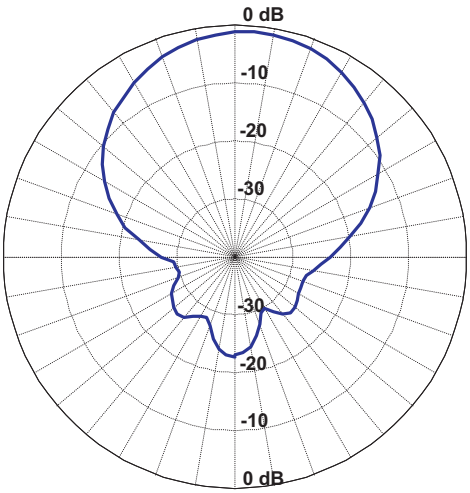

(c) 9mm separation distance, no dielectric

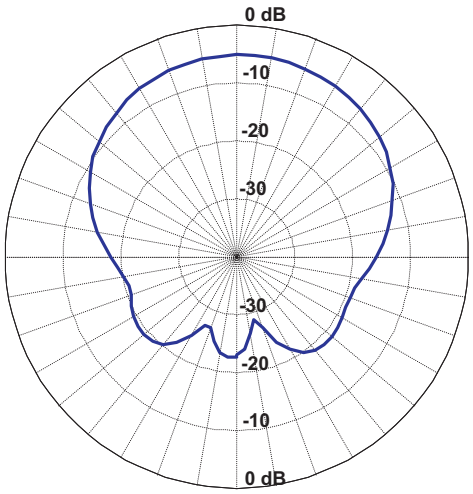

(d) 9mm separation distance, with dielectric

Figure 27: The standard 915MHz dipole antenna made of milled copper gain patterns with and without the graduated dielectric spacer.

A.2 Medium Trace Width, Wide Separation Distance Design

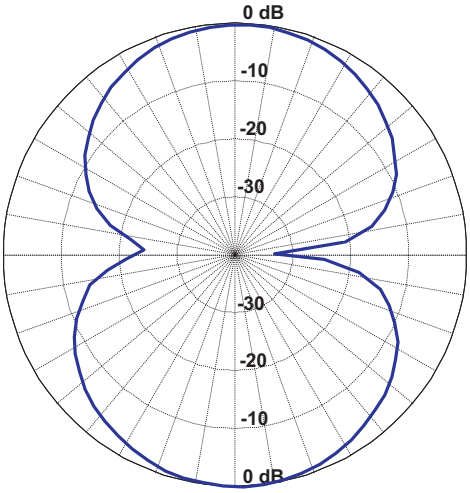

(a) Free space.

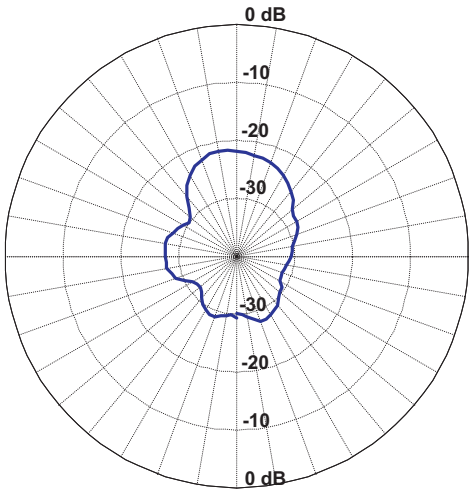

(b) FR4 directly on ground plane.

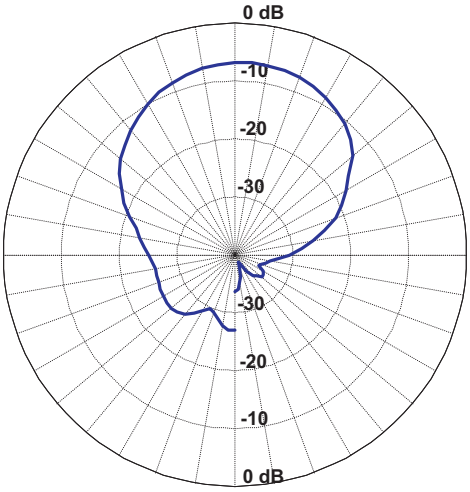

(c) 3mm separation distance, no dielectric

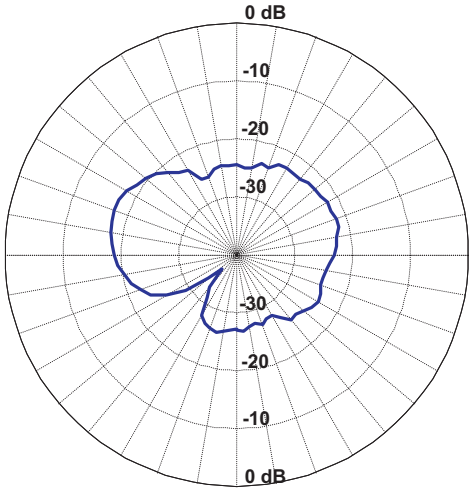

(d) 3mm separation distance, with dielectric

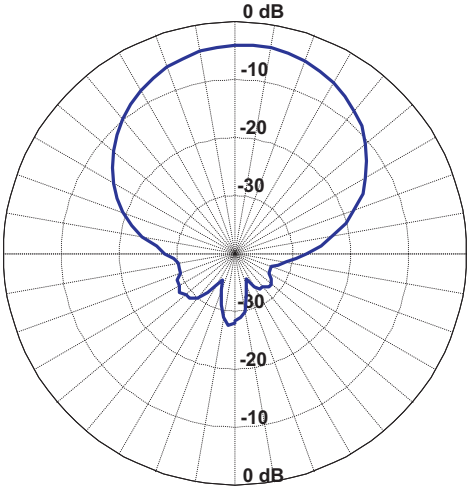

(a) 6mm separation distance, no dielectric

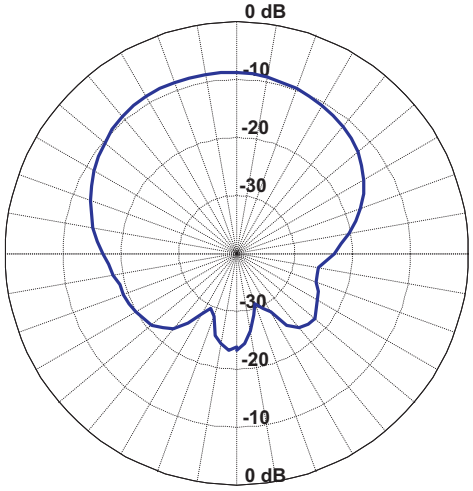

(b) 6mm separation distance, with dielectric

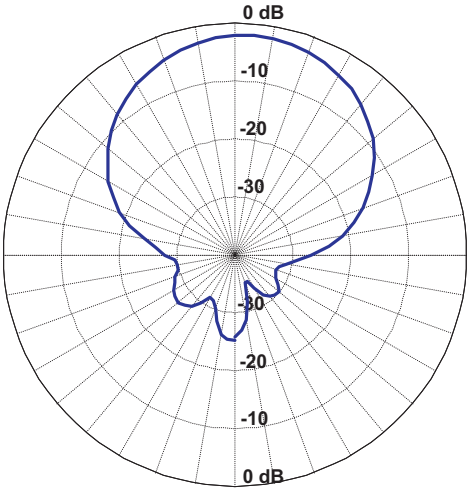

(c) 9mm separation distance, no dielectric

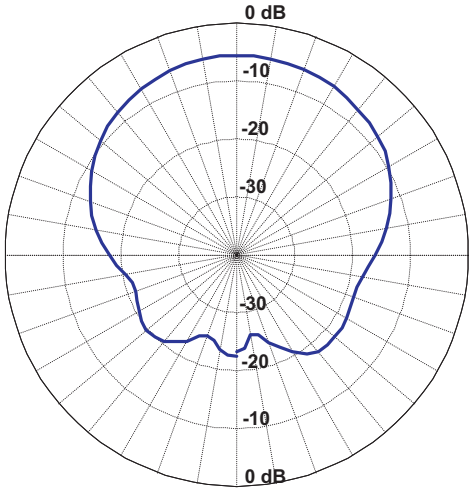

(d) 9mm separation distance, with dielectric

Figure 28: The medium trace width, wide separation distance 915MHz dipole antenna made of milled copper gain patterns with and without the graduated dielectric spacer.

A.3 Medium Trace Width, Medium Separation Distance Design

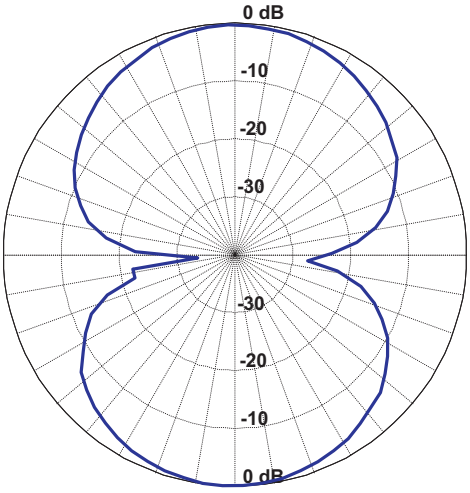

(a) Free space.

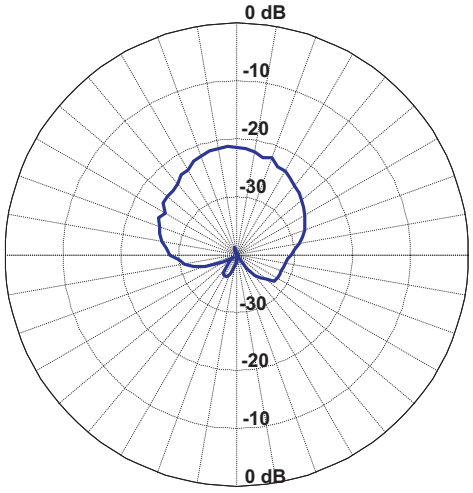

(b) FR4 directly on ground plane.

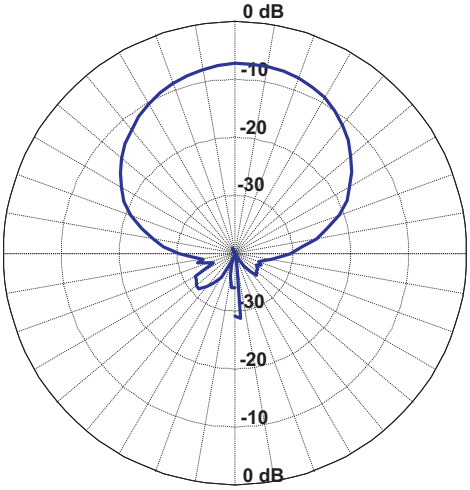

(c) 3mm separation distance, no dielectric

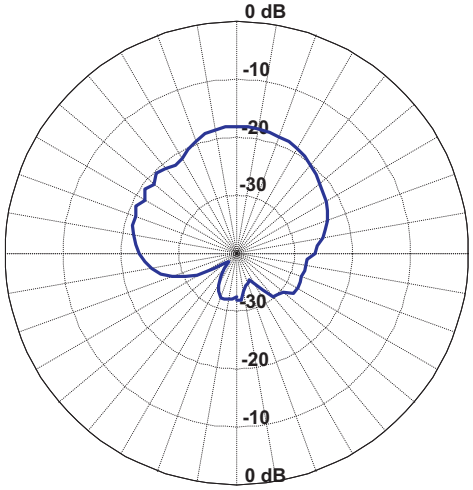

(d) 3mm separation distance, with dielectric

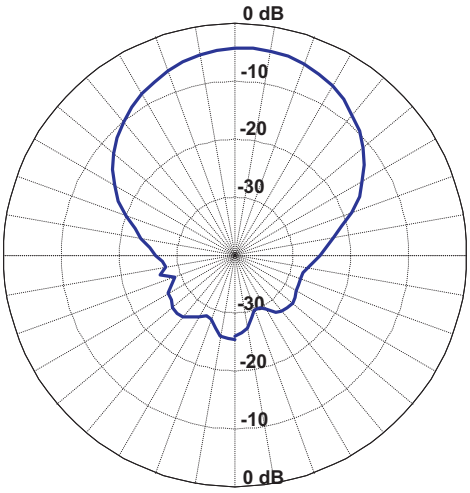

(a) 6mm separation distance, no dielectric

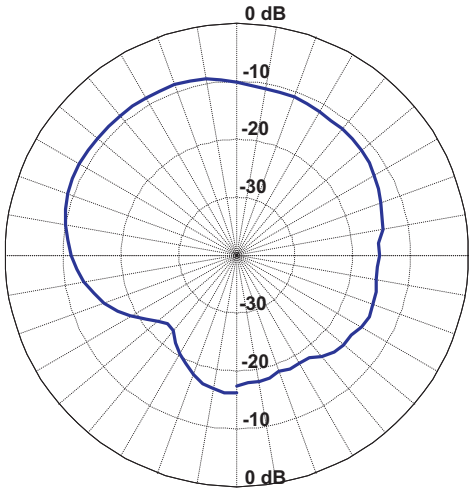

(b) 6mm separation distance, with dielectric

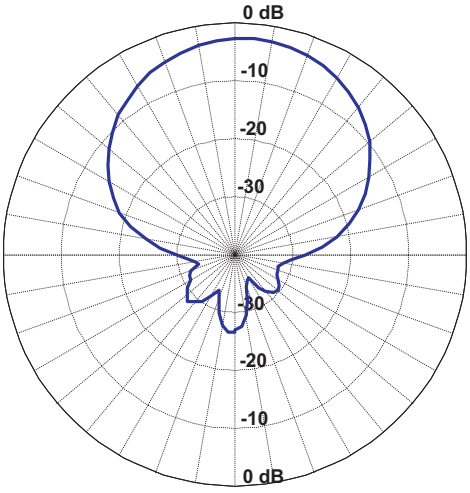

(c) 9mm separation distance, no dielectric

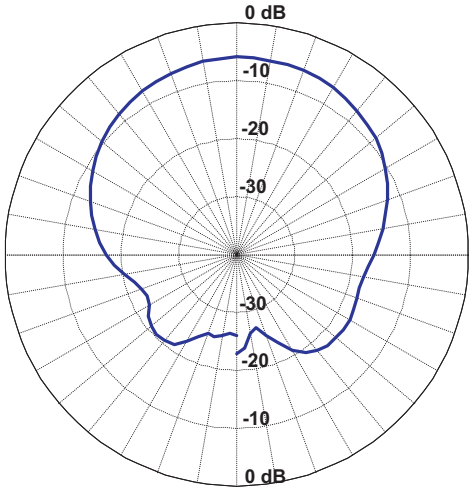

(d) 9mm separation distance, with dielectric

Figure 29: The medium trace width, medium separation distance 915MHz dipole antenna made of milled copper gain patterns with and without the graduated dielectric spacer.

A.4 Medium Trace Width, Small Separation Distance

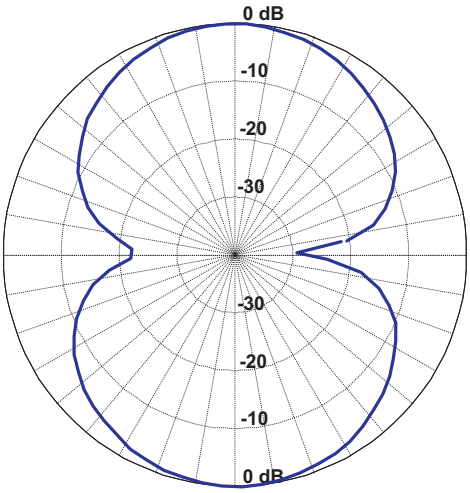

(a) Free space.

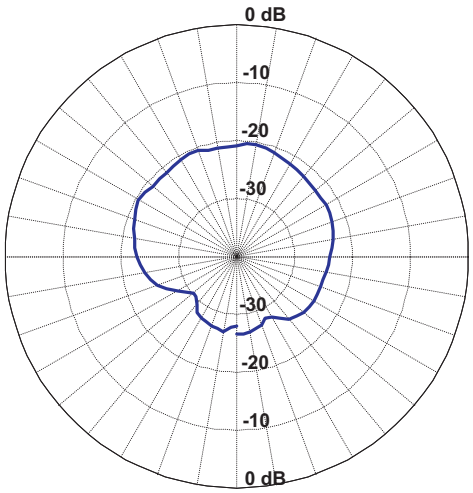

(b) FR4 directly on ground plane.

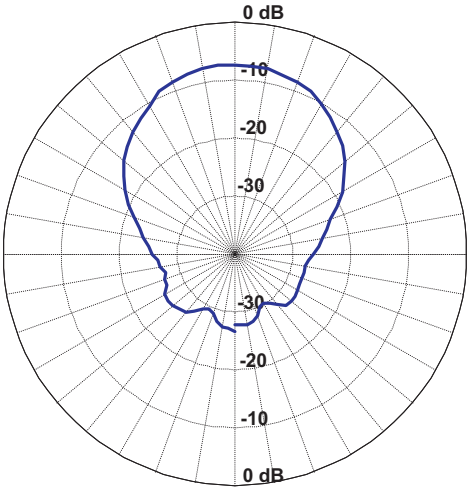

(c) 3mm separation distance, no dielectric

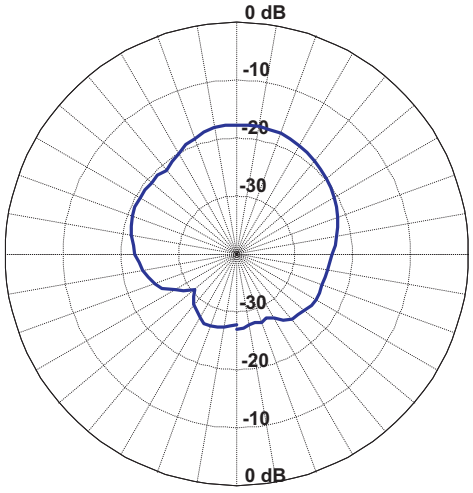

(d) 3mm separation distance, with dielectric

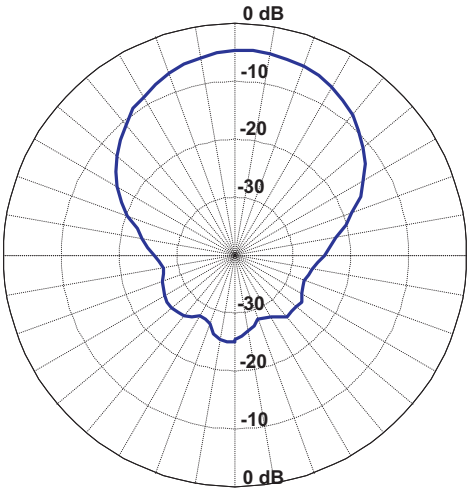

(a) 6mm separation distance, no dielectric

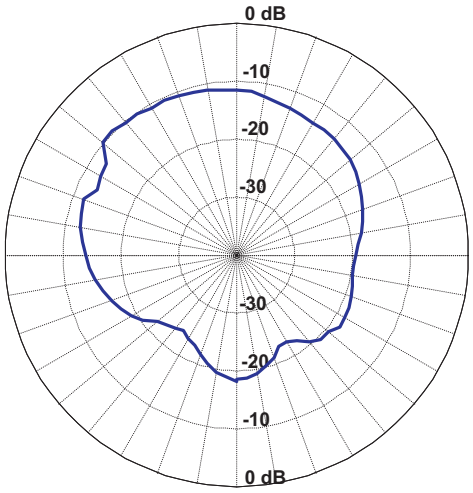

(b) 6mm separation distance, with dielectric

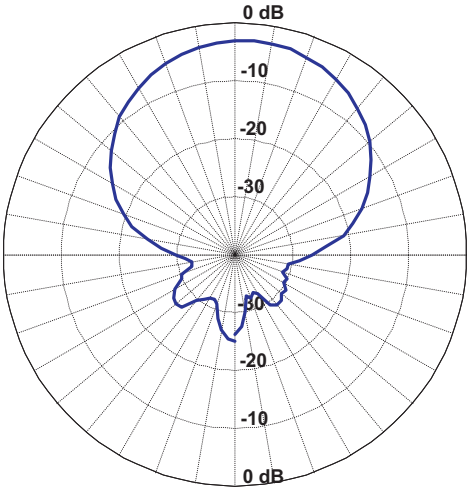

(c) 9mm separation distance, no dielectric

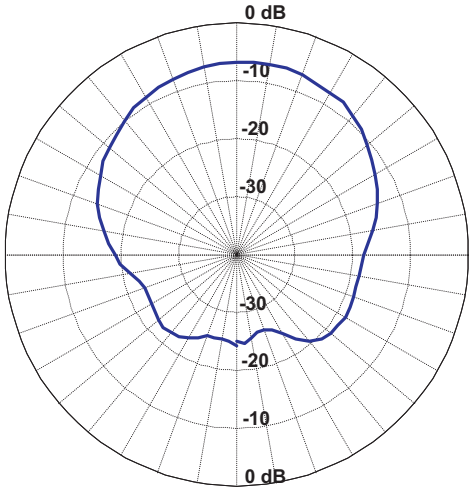

(d) 9mm separation distance, with dielectric

Figure 30: The medium trace width, small separation distance 915MHz dipole antenna made of milled copper gain patterns with and without the graduated dielectric spacer.

A.5 Thin Trace Width Design

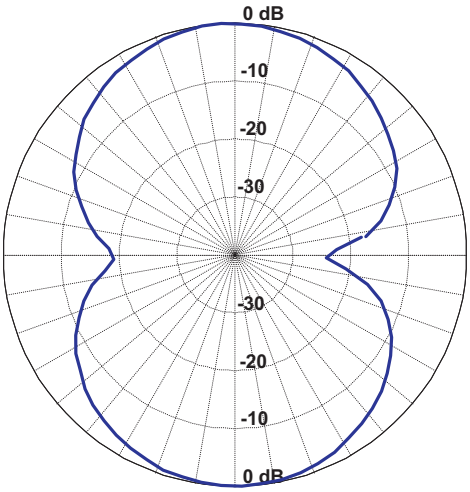

(a) Free space.

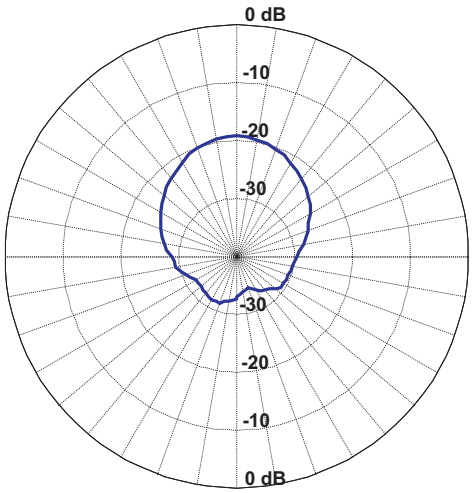

(b) FR4 directly on ground plane.

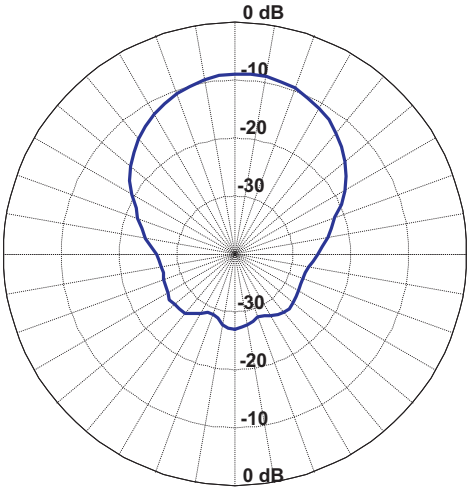

(c) 3mm separation distance, no dielectric

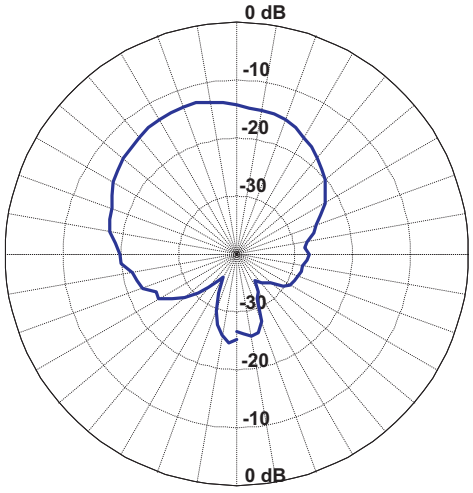

(d) 3mm separation distance, with dielectric

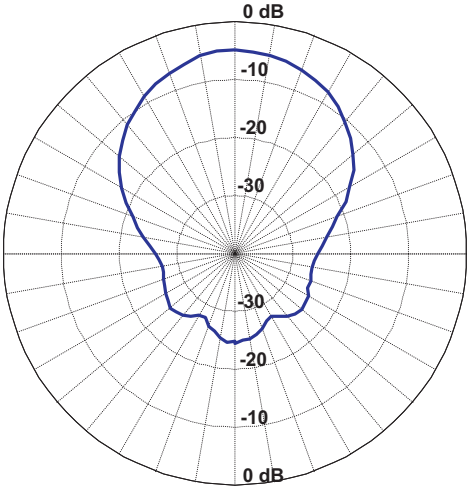

(a) 6mm separation distance, no dielectric

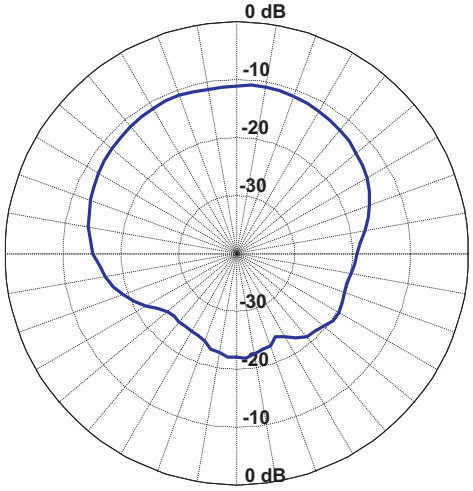

(b) 6mm separation distance, with dielectric

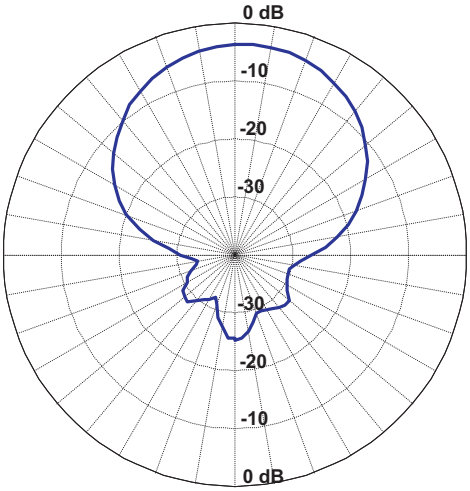

(c) 9mm separation distance, no dielectric

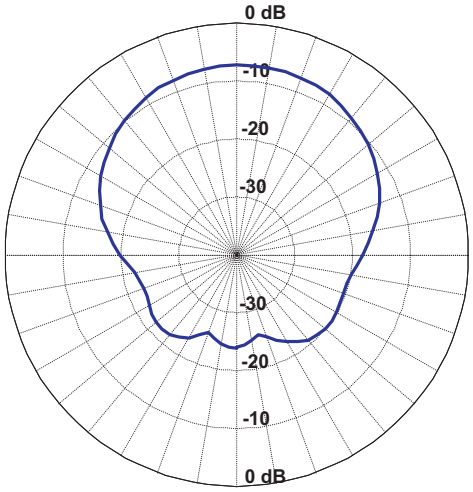

(d) 9mm separation distance, with dielectric

Figure 31: The thin trace width, wide separation distance 915MHz dipole antenna made of milled copper gain patterns with and without the graduated dielectric spacer.

APPENDIX B

DE-EMBEDDING THE BALUN

De-embedding the balun transformer required measuring the balun with the network analyzer with an open, short, and matched load. Using (25), (26) and (27), and assuming the balun is reciprocal ($S_{21} = S_{12}$), the s-parameters for the balun can be obtained. Case 1: The S_{11} measurement when the balun is terminated by a matched load.

$$\Gamma_{50\Omega} = S_{11} \tag{25}$$

Case 2: The S_{11} measurement when the balun is terminated by a short circuit.

$$\Gamma_{SC} = S_{11} - \frac{S_{12}S_{21}}{1 + S_{22}} \tag{26}$$

Case 3: The S_{11} measurement when the balun is terminated by an open circuit.

$$\Gamma_{OC} = S_{11} + \frac{S_{12}S_{21}}{1 - S_{22}} \tag{27}$$

Now there are three equations for three unknown s-parameters. Once the s-parameters are found, the balun transfer can be de-embedded to find the actual impedance of the antenna.

REFERENCES

[1] Best, S. R. and Hanna, D., "A Broadband Planar Folded Dipole Over an EBG Ground Plane," *USNC/URSI National Radio Science and AMEREM Meetings*, p. 221, July 2006.

[2] Choi, W., Seong, N.-S., Kim, J. M., Pyo, C., and Chae, J., "A Planar Inverted-F Antenna (PIFA) to be Attached to Metal Containers for an Active RFID Tag," *IEEE Antennas and Propagation Society International Symposium*, vol. 1B, pp. 508–511, July 2005.

[3] Dobkin, D. M. and Weigand, S. M., "Environmental Effects of RFID Tag Antennas," *IEEE MTT-S International Microwav Symposium Digest*, pp. 12–17, 2005.

[4] EPC Global, *Protocal Specification for 900 MHz RFID Tag.*

[5] Griffin, J., Durgin, G., Haldi, A., and Kippelen, B., "How to Contruct a Test Bed for RFID Antenna Measurements," *IEEE Antennas and Propagation Society International Symposium*, pp. 457–460, July 2006.

[6] Griffin, J., Durgin, G., Haldi, A., and Kippelen, B., "RF Tag Antenna Performance on Various Materials Using Radio Link Budgets," *IEEE Antennas and Propagation Letters*, vol. 5, pp. 247–250, Dec. 2006.

[7] Karthaus, U. and Fischer, M., "Fully Integrated Passive UHF RFID Transponder IC with 16.7-/spl mu/W Minimum RF Input Power," *IEEE Journal of Solid-State Circuits*, vol. 38, pp. 1602–1608, Oct 2003.

[8] Ma, K. P., Hirose, K., Yang, F. R., Qian, Y., and Itoh, T., "Realisation of Magnetic Conducting Surface Using Novel Photonic Bandgap Structure," *Electronics Letters*, vol. 34, pp. 2041–2042, Oct 1998.

[9] Nikitin, P. V. and Rao, K. V. S., "Performance Limitations of Passive UHF RFID Systems," pp. 1011–1014, July 2006.

[10] Ollivier, M. M., "RFID-A Practical Solution to Problems You Didn't Even Know You Had!," *IEE Colloquium on Wireless Technology*, Nov. 1996.

[11] Orton, R. S. and Seddon, N. J., "PMC as an antenna structural component," *Twelfth International Conference on Antennas and Propagation.*

[12] Rahmat-Samii, Y. and Mosallaei, H., "Electromagnetic Band-gap Structures: Classification, Characterization, and Applications," *Eleventh International Conference on Antennas an Propagation*, vol. 2, pp. 560–564, April 2001.

[13] Rao, K., Nikitin, P., and Lam, S., "Antenna Design for UHF RFID Tags: A Review and a Practical Application," *IEEE Transactions on Antennas and Propagation*, vol. 53, pp. 1370–1376, Dec. 2005.

[14] Raumonen, P., Sydanheimo, L., Ukkonen, L., Keskilamm, M., and Kivikoski, M., "Folded Dipole Antenna Near Metal Plate," *Antennas and Propagation Society International Symposium*, 2003.

[15] Rudge, A. W., Milne, K., Olver, A. D., and Knight, P., *The Handbook of Antenna Design*. IET, May 1986.

[16] Sidén, J., Nilsson, H. E., Koptyug, A., and Olsson, T., "A Distanced RFID Dipole for a Metallic Supply Chain Label," *IEEE Antennas and Propagation Society International Symposium*, pp. 3229–3232, July 2006.

[17] Smith, G. S., *An Introduction to Classical Electromagnetic Radiation*. Cambridge, United Kingdom: Cambridge University Press, 1997.

[18] Ukkonen, L., Sydänheimo, L., and Kivikoski, M., "Effects of Matallic Plate Size on the Performance of Microstrip Patch-Type Tag Antennas for Passive RFID," *IEEE Antennas and Wireless Propagation Letters*, vol. 4, pp. 410–413, 2005.

[19] Yu, B., Kim, S. J., Jung, B., Harackiewicz, F. J., Park, M. J., and Lee, B., "A Distanced RFID Dipole for a Metallic Supply Chain Label," *IEEE Antennas and Propagation Society International Symposium*, pp. 3237–3240, July 2006.